https://doi.org/10.5194/egusphere-2024-3976
Preprint. Discussion started: 21 January 2025

Uncertainties in OCO-2 satellite retrievals of XCO_2 limit diagnosis of transport model simulation uncertainty

Chiranjit Das[1], Ravi Kumar Kunchala[1], Prabir K. Patra[2,3], Naveen Chandra[2], Kentaro Ishijima[4], Toshinobu Machida[5]

[1] Centre for Atmospheric Sciences, Indian Institute of Technology Delhi, New Delhi, India
[2] Japan Agency for Marine-Earth Science and Technology (JAMSTEC), Yokohama 236-0001, Japan
[3] Research Institute for Humanity and Nature, Kyoto 6038047, Japan
[4]Meteorological Research Institute, Tsukuba, Japan
[5]National Institute for Environmental Studies, Tsukuba, Japan

Correspondence to: Prabir K. Patra (prabir@jamstec.go.jp) and Chiranjit Das (Chiranjit.Das@cas.iitd.ac.in)

Abstract. Estimating regional CO_2 sources and sinks is challenging due to limited data and uncertainties in transport models. Orbiting Carbon Observatory-2 (OCO-2) overcomes measurement limits, providing CO_2 variations beyond in-situ networks. This study analyses altitude-wise model-observation CO_2 differences from surface to upper troposphere using aircraft observations from ATom, Amazon, and CONTRAIL campaigns over OCO-2 total column CO_2 (XCO_2) sampling location to characterise sources of uncertainty in MIROC4-ACTM. We show model aligns better with ATom tropospheric columns (0.03 ± 0.03 ppm) than OCO-2 XCO_2 (0.2 ± 0.5 ppm), especially over oceans, highlighting the need for expanded profile measurements to characterise errors robustly. Altitude-wise comparisons reveal this differences primarily occur in the lower troposphere (0-2 km), likely due to ACTM's near-surface land CO_2 flux errors. In contrast, ACTM better matches aircraft CO_2 in the middle (2-5 km) and upper (5-8 km) troposphere, likely due to accurate large-scale transport representation. Over the Amazon, CO_2 differences with aircraft and OCO-2 differ, likely due to a lack of regional surface sites for inversion and insufficient high-altitude profile (~4km) not representative of XCO2. Over Asian megacity airports, which are significant emission hotspots, the model shows a large negative difference with CONTRAIL than OCO-2. This discrepancy likely hints that MIROC4-ACTM is unable to capture urban fossil CO_2 emission signals at airports due to coarse resolution (~2.8° x 2.8°) and higher resolution of OCO-2 limits ability to fully capture actual emission footprints.

Keywords: Carbon dioxide; Aircraft; Transport Model; OCO-2

https://doi.org/10.5194/egusphere-2024-3976
Preprint. Discussion started: 21 January 2025

1. Introduction

Atmospheric CO_2 is the most significant anthropogenic greenhouse gas (GHG) present in the Earth's atmosphere, responsible for a major global warming and climate change since the preindustrial era, circa 1750 (Canadell et al., 2022). Therefore, recognizing its importance in direct impact on climate, monitoring of highly accurate surface CO_2 measurements were first started from the South Pole (SPO) and Mauna Loa (MLO), Hawaii (Keeling, 1960) and later expanded across the globe. These in-situ measurements are widely used for estimating surface CO_2 fluxes using Bayesian-based "top-down" chemistry transport models due to their long-term record and high measurement accuracy (Chandra et al., 2022; Chevallier et al., 2010; Peylin et al., 2013). However, in-situ CO_2 measurement sites around globe is sparse, mostly situated in mid-latitude north America and Europe, with less coverage over tropical land (Patra et al., 2011; Schimel et al., 2015) and open oceans, which increase difficulties in inferring surface CO_2 fluxes from inverse models in data void regions (Chevallier et al., 2010, 2011).

To increase spatiotemporal monitoring of CO_2, spaced-based measurements such as SCanning Imaging Absorption spectroMeter for Atmospheric CartograpHY (SCIAMACHY), Greenhouse Gases Observing Satellite "IBUKI" (GOSAT), and the Orbiting Carbon Observatory-2 (OCO-2) were launched to provide column-average dry-air mole fraction or mixing ratio of CO_2, termed XCO_2 (Bovensmann et al., 1999; Crisp, 2008; Kuze et al., 2009). NASA's OCO-2 satellite launched in 2014 to achieve finer spatial resolution and better precision as compared to previous satellites. This advancement has proved beneficial for understanding global and regional carbon cycle science in various satellite based studies (Crisp, 2015; Das et al., 2023; Liang et al., 2017; Liu et al., 2017; Chatterjee et al., 2027). OCO-2 version 10 XCO_2 measurements has shown retrieval error with mean bias (RMSE) of 0.24 (0.81) ppm over land and 0.43 (0.84) ppm over ocean globally, compared against more accurate WMO scale maintained XCO_2 from surface-based Total Carbon Column Observation Network (TCCON) sites (Taylor et al., 2023; Wunch et al., 2017). Studies reported that assimilation of OCO-2 XCO_2 available at greater spatial density (~ 100 times of GOSAT) into an inversion requires the data to be extremely precise, stable and regionally unbiased to effectively estimate surface CO_2 fluxes in regional scale (Byrne et al., 2017, 2023; Crowell et al., 2019; Philip et al., 2022; Rastogi et al., 2021). Also, Miller et al. (2007) reported that satellite-retrieved XCO_2 needs regional precision of 1-2 ppm to reduce uncertainty in inversion-derived flux estimates from in-situ networks. Because, XCO_2 retrievals having many sources of uncertainty hinder their fidelity to utilize inversion approach to accurately estimate surface CO_2 flux (Chevallier et al., 2014; Villalobos et al., 2020). These retrieval errors in OCO-2 include cloud effects (Massie et al., 2021;Merrelli et al., 2015), instrumental errors, retrieved surface pressure, and then aerosol, the largest source of systematic error can be approximately 2 ppm over land regions (Connor et al., 2016). Therefore, to enhance the accuracy of surface CO_2 flux estimations, studies are focussing on improving retrieval algorithm by correcting for cloud effects and incorporating a digital elevation model (DEM) to correct surface pressure (Jacobs et al., 2023; Mauceri et al., 2023). Apart from retrieval errors, misrepresentation of transport and uncertainty in prior fluxes can further reduce reliability in top-down model inferred surface CO_2 fluxes (Chandra et al., 2022; Fu et al., 2021; Schuh et al., 2019). To address and assess such kind of errors impact on top-down CO_2 budgets, OCO-2 model intercomparison project (MIP) is formed with different CO_2 inverse modelling groups assimilating OCO-2, in-situ and combination of both (https://gml.noaa.gov/ccgg/OCO2_v10mip/index.php).

https://doi.org/10.5194/egusphere-2024-3976
Preprint. Discussion started: 21 January 2025

Previous studies have attempted to reconstruct observation based CO_2 profiles combining ship, aircraft and model simulation to compare with GOSAT XCO_2, but are limited to characterise inversion errors (Müller et al., 2021; Inoue et al., 2013; Wofsy, 2011). Frankenberg et al. (2016), showed using HIPPO aircraft CO_2 vertical profiles, that the retrievals of GOSAT, TES, AIRS satellites and inversion simulation can have large difference of ~ 4 ppm due to inaccurate vertical transport in higher latitude during vegetation growing or decaying periods. These studies often lack in providing uncertainties linked with inversion through altitude-based CO_2 comparison from near surface to different tropospheric layers between inversion-based model simulations, surface, and aircraft data. This gap is particularly evident in regions with in-situ sparse data coverage, such as vast oceanic areas, as well as in emission or sink hotspots over land while OCO-2 dense measurements have not helped to overcome precision issues providing global coverage. However, no studies attempted to understand how OCO-2 retrieval errors or accuracy hampers its full potential to uncover the uncertainties associated with inverse models. The present study aims to understand sources of error associated with the MIROC4-ACTM model through altitude-based CO_2 comparison among MIROC4-ACTM, OCO-2 and aircraft observation across different tropospheric layers. To accomplish this we leverage highly accurate and precise aircraft vertical CO_2 measurements from ATom campaigns over northern America, Pacific, Atlantic, Southern Ocean regions, CONTRAIL over airports in Asia and four specific sites in Amazon. Before analysing, we first validated the MIROC4-ACTM model simulated tropospheric column CO_2 (XCO_2) with highly precise CO_2 vertical profiles from independent aircraft measurements over open oceanic regions, Amazon and local urban hotspot over Asia.

2. Data and Methodology

2.1 Aircraft and surface CO_2 measurements

We have used individual independent aircraft and surface in-situ CO_2 measurements around the globes from NOAA's obspack_co2_1_GLOBALVIEWplus_v8.0 data product (Schuldt et al., 2022) and WDCGG (World Data Centre for Greenhouse Gases) respectively. We have selected a few individual campaigns such as ATom, Amazon aircraft campaigns, CONTRAIL because of their extensive latitudinal/longitudinal spatial coverage over ocean and land regions, multiple vertical CO_2 profile measurements and extended period of measurements. A brief description of each aircraft measurement is discussed in the next paragraphs.

ATom is an aircraft field campaign, providing airborne measurements of remote tropospheric and lower stratospheric CO_2 from Northern America, Arctic, Pacific, Southern and Atlantic Oceans (Thompson et al., 2022). ATom has four campaigns conducted using NASA DC-8 aircraft, taking vertical profile of CO_2 from near surface (0.15 km) to13 km altitude range over four seasons from 2016 to 2018. Four campaigns each lasted around 28 days, namely, ATom–1, 28 July-22 August 2016; ATom–2, 26 January–22 February 2017; ATom–3, 28 September–26 October 2017; ATom–4, 24 April to 21 May 2018 respectively (Wofsy et al., 2021). These vertical CO_2 measurements enable the validation of XCO_2 measurements from the satellites because most of XCO_2 variability is constrained in the troposphere, therefore, these vertical measurements effectively serve as a reference for satellite-retrieved CO_2 validation (Frankenberg et al., 2016). We have utilised these CO_2 measurements freely available at https://gml.noaa.gov/ccgg/obspack/data.php.

https://doi.org/10.5194/egusphere-2024-3976
Preprint. Discussion started: 21 January 2025

Additionally, aircraft vertical campaign CO_2 measurements from four sites such as TEF (3.39° S, 65.6° W), SAN (2.86° S, 54.95° W), RBA (9.38° S, 67.62° W) and ALF (8.80° S, 56.75° W) in the Amazon region are also considered for the present study and more details about these measurements can be found in Gatti et al. (2021a). In ALF, RBA, SAN, CO_2 measurements are available from 2010 to 2018, whereas TEF has measurements from 2013-2018. Bi-monthly vertical CO_2 profile measurements were taken during 12:00 and 13:00 local time at all these sites covering altitude from 0.3 to 4 km when the daytime boundary layer is well mixed. These measurements were taken using an automatic sampler onboarded in the light aircraft, which underwent accuracy and precision testing at greenhouse gas laboratory at National Institute of Space Research (LaGEE/INPE), Brazil (Gatti et al. 2014). We have used a set of vertical CO_2 profiles during September, 2014 till 2018, freely available at: https://doi.pangaea.de/10.1594/PANGAEA.926834 (Gatti et al., 2021b).

Further, CONTRAIL aircraft program CO_2 measurements over Asian regions are also considered for the current analysis (Ishijima et al., 2021; Machida et al., 2008; Matsueda et al., 2008). In this program, several regular passenger aircraft operated by Japan Airlines (JAL) are installed with instruments like CME (Continuous CO_2 Measuring Equipment) to provide extensive spatial CO_2 data coverage in the upper troposphere and lower stratosphere (UT/LS) region. We have only considered measurements during OCO-2 measurements period at four representative zones in Asia, specifically around airports, to retrieve vertical CO_2 profiles during ascent or descent of the aircraft, following Niwa et al., 2011. The measurements dataset is freely accessible at https://www.cger.nies.go.jp/contrail/.

2.2 OCO-2

OCO-2 is a sun-synchronous satellite, retrieves XCO_2 to understand the carbon source-sink activity throughout the globe (Eldering et al., 2017). The satellite uses three high-resolution grating spectrometers to retrieve the reflected sunlight spectral signature of weak CO_2 (1.61 μm), strong CO_2 (2.06 μm) and O_2A (0.76 μm) which are later analysed through Atmospheric Carbon Observations from Space (ACOS) algorithm to estimate global spatiotemporal XCO_2 distribution (Crisp, 2015; Crisp et al., 2017; Eldering et al., 2017). It has a spatial resolution of 1.29 km × 2.25 km (nadir mode), and a temporal periodicity of sixteen days. We have utilised OCO-2 version 10 which is an update from previous version v8/v9 in terms of important changes in spectroscopy, aerosol, CO_2 prior source, and solar continuum model which reduced RMSE validated against XCO_2 measured at TCCON sites for land and ocean-glint measurement (Taylor et al., 2023). In this study, we have used level–2 OCO-2 version 10r data product (available at: https://disc.gsfc.nasa.gov/datasets/OCO2_L2_Standard_10r/summary?keywords=OCO-2) and have considered only bias-corrected quality checked soundings (XCO_2_quality_flag = 0 or good data) for analysis.

2.3 Transport model

The Model for Interdisciplinary Research on Climate, version 4, based Atmospheric Chemistry Transport Model (MIROC4–ACTM) chemistry transport model is used, which is run at T42 spectral spatial resolution (~2.8° × 2.8° latitude-longitude grid) with 67 vertical hybrid-pressure levels from the surface to 90 km to simulate the CO_2

https://doi.org/10.5194/egusphere-2024-3976
Preprint. Discussion started: 21 January 2025

concentration and fluxes (Patra et al., 2018). For realistic representation of the transport in the model, model meteorology, horizontal winds (zonal and meridional) and temperature is nudged to Japanese 55-year Reanalysis or JRA-55 data (Kobayashi et al., 2015). The MIROC4-ACTM model conducted two distinct simulations: one utilizing bottom-up model a prior or "FG" fluxes and the other employing a posteriori or "InvFG" fluxes derived from top-down inversion using 50 inversion sites (Figure S1). To derive total concentration in the simulation different bottom-up tracers are utilised, gridded GridFED fossil fuel; $CO_{2,ff}$ (Jones et al., 2021), annually balanced CASA biospheric flux; $CO_{2,lnd}$ (Randerson et al., 1997) and ocean exchange i.e., sea-air CO_2 flux; $CO_{2,ocn}$ (Takahashi et al., 2009). Then, prior CO_2 simulation case of MIROC4-ACTM is prepared by adding the prior tracers as follows: $CO_{2,ff}$ (GridFED) + $CO_{2,lnd}$ (CASA–3hr) + $CO_{2,ocn}$ (Taka–Ocn). A detailed discussion on this is given in Chandra et al. 2022. Further, to minimise the edge effect on the simulated dataset, we discarded the first two years and last one year of our simulation period (2012-2022), only analysed CO_2 of both simulation and observation during 2014-2021. Model performance evaluated by comparing with each vertical profile of independent observations of ATom CO_2 not used in the inversion as well as at two surface sites, MLO (19.53 °N, 155.57 °W) and SYO (69.01 °S, 35.59 °W) representative of northern and southern hemisphere CO_2 variability (Fig. S2, 3). To do that firstly, model simulated CO_2 is resampled to the nearest grid of the aircraft and surface sampling locations, considering linear interpolations at spatial grid and time. We have not considered any other co-location criteria unless it is mentioned, e.g., geometric and dynamic for comparison; therefore, estimated CO_2 difference is essentially uncertainty either in observation or inversion (Kulawik et al., 2016, 2019). The result shows good performance with lesser bias with InvFG over prior at different latitudes, showing an overall good match of InvFG CO_2 and ATom at different latitudes (Fig. S2, 3). Similarly at surface sites, InvFG showed better performance over prior with correlation of 0.99 with observation ($p < 0.05$) (Fig. S4). Then, to compare OCO-2 XCO_2 and ACTM-XCO_2, we formulated XCO_2^{ACTM} following the Patra et al., 2017. Here, ACTM simulated CO_2 profile or CO_2^{ACTM} resampled at each OCO-2 retrieval location (latitude, longitude) with further use of corresponding OCO-2 priori and column average kernel sensitivity (Ai) represents instrumental sensitivity for 20 vertical levels from top of atmosphere (TOA) to surface to produce XCO_2^{ACTM} using the following equation.

$$XCO_2^{ACTM} = \sum_i (CO_2^{priori} \cdot dP_i) + \sum_i A_i \cdot dP_i \left(\sum_i CO_2^{ACTM_i} - \sum_i CO_2^{priori}\right) \quad (1)$$

CO_2^{priori} = OCO-2 priori; A_i = OCO-2 column averaging kernel; dP_i = thickness of each pressure layer.

We have also resampled XCO_2^{ACTM} at 21 TCCON sites around the globe to validate model performance with more accurate XCO_2 measurements at surface-based TCCON sites (Wunch et al., 2011). To perform that we first filtered data points considering only good quality retrieval, then curve fitted the remaining retrieval to remove outliers and finally considered retrievals with solar zenith angle < 60° following methodology mentioned in Appendix C of Crowell et al. 2019. Figure S5 shows a good agreement between ACTM and TCCON XCO_2 for majority of TCCON sites considering the fact that TCCON has its own bias due to topography, surface brightness and aerosols as well as latitudinal varying bias (Wunch et al., 2017).

2.4 Data analysis

https://doi.org/10.5194/egusphere-2024-3976
Preprint. Discussion started: 21 January 2025

To conduct the spatial discrepancy analysis of XCO_2 difference between ACTM and OCO-2, bias corrected and quality checked good soundings from OCO-2 XCO_2 retrieval or $XCO_2^{OCO\text{-}2}$ and ACTM simulated XCO_2 or XCO_2^{ACTM} is re-gridded into $0.5° \times 0.5°$ latitude-longitude grid boxes. Further, to assess this XCO_2^{ACTM} - $XCO_2^{OCO\text{-}2}$ difference, we used aircraft vertical CO_2 measurement available at different vertical tropospheric layers, essentially to conduct an altitude-wise comparison of CO_2 among ACTM, OCO-2 and aircraft. Therefore, we have employed a methodology outlined using a schematic in Figure 1, specifically designed to provide CO_2 profile from aircraft, OCO-2 and ACTM.

It shows typical CO_2 concentration vertical profiles and relative altitude range captured in OCO-2, aircraft measurements, and corresponding MIROC4-ACTM simulations. OCO-2 measures XCO_2 concentration from space, representing CO_2 profile from top of the atmosphere to surface so as the ACTM simulation at those pressure levels is represented by a blue colour double-headed arrow. On the other hand, aircraft tropospheric columns of CO_2 typically capture concentration variability up to an altitude of 15 km and ACTM resampled concentration values at those measurement locations represented by orange colour double headed arrows. Since the main purpose is to compare the aircraft tropospheric column CO_2 against OCO-2 XCO_2 and ACTM simulations, we subdivided the tropospheric CO_2 column into three different vertical tropospheric layers, namely, the lower troposphere: lowest level to 2 km, middle troposphere: 2–5 km, and upper troposphere: 5–8 km to understand the model performance in each of the vertical layers. In addition, a total tropospheric vertical CO_2 column of aircraft or aircraft XCO_2 is calculated only when the vertical measurements reach at least 8 km altitude; otherwise, any profile not reaching 8 km is discarded from the analysis unless otherwise mentioned specifically. For each vertical tropospheric layer, pressure-weighted partial column CO_2 is calculated to consider air mass variation between pressure levels for each considered tropospheric layer. Moreover, to become more robust on the analysis, each vertical depth layer is subdivided into 200 bins unless otherwise mentioned and 80% of vertical bins having measurements for the specific tropospheric layer only considered for analysis. For instance, middle troposphere (upper troposphere), i.e., 2–5 (5–8) km is divided into 15 vertical bins each of 200 meters, then in a specific latitude or longitude while calculating a partial column of CO_2, we only considered profiles that encompass a minimum 12 vertical bins in them.

3. Results

3.1. MIROC4-ACTM intercomparison with OCO-2 and surface measurements

Figure 2a shows a monthly mean spatial XCO_2 difference (XCO_2^{ACTM} - $XCO_2^{OCO\text{-}2}$) during January, 2015 – December, 2021. It reveals a heterogeneous signature of spatial XCO_2 difference or mismatch across the globe with maximum negative XCO_2 difference of approximately 2 ppm over Amazon, Africa, south-east Asia, China, primarily in the global tropical land regions. This is likely due to the lack of long-term surface CO_2 measurements (Figure S1) available for inversion particularly over the global tropics to constrain the prior CO_2 flux (also discussed in Chandra et al., 2022). Further, humid tropics is also the region of lesser valid OCO-2 retrievals due to the persistent shallow cumulus cloud blocking the infrared signals, makes it challenging to validate the transport model and studies has shown sparse sampling over land increases chances of the error almost two times (Frankenberg et al., 2024; Kulawik et al., 2019). On the other hand, high-latitude land regions, North America

https://doi.org/10.5194/egusphere-2024-3976
Preprint. Discussion started: 21 January 2025

and Russia, exhibit a positive XCO_2 difference of nearly 2 ppm, however, XCO_2 differences over ocean regions are generally within ± 1 ppm, possibly because of lesser variability in ocean CO_2 flux compared to land CO_2 flux and oceanic regions are minimally affected by land air mass. Further, we observed a negative XCO_2 difference especially over northern extra-tropics between 30° N to 60° N of nearly -0.6 ppm in agreement with Byrne et al. 2023 likely attributed to OCO-2 ocean glint (OG) retrieval biases that adds up a layer of complexity of diagnosing the transport model against OCO-2 retrievals over this vast ocean. Further, studies showed that sampling variance between land and ocean could also lead significant uncertainty (Basu et al., 2018). Additionally, we observed a bias in the Southern Hemisphere, the underlying causes of which are still unknown and need further research (Byrne et al., 2023). Overall, our results show some regions under/over-estimated by ACTM, however, it is challenging to comprehend quantitatively and qualitatively about sources of error across diverse regions (source-sink dynamics and transport mechanism) as it could result either due to inaccuracies in the inversion (prior fluxes, transport) or errors in satellite retrievals (Chandra et al., 2022; Chevallier et al., 2014). Furthermore, to check the time variation of these XCO_2 differences, we analysed the time versus latitude distribution of XCO_2 difference taking the average across global longitude from 180° W to 180° E (Fig. 2b). We observed that XCO_2 difference has a seasonal and spatially varying repeating signature, with maximum (minimum) difference during February-March-April (September-October-November) consistent across study period. A prominent positive (negative) systematic XCO_2 difference is observed over the southern hemisphere tropic to mid-latitude from 10° S–40° S and northern latitude around 30° N (northern tropic to mid latitude) this is in agreement with Kulawik et al. (2019). However, after separating time vs latitude distribution of XCO_2 difference into land and ocean, we observed that this systematic XCO_2 difference mainly originates from the southern ocean part, which matches well with overall (land and ocean) time vs latitude XCO_2 difference distribution (Fig. S6). However, it is challenging to explain the difference since ocean glint has biases (Byr ne et al., 2023) and a study by Kulawik et al. (2019) also reported a systematic error of 0.6 ± 0.1 ppm could arise over the ocean and land in OCO-2 satellite XCO_2 retrievals.

To further examine whether this difference comes from inversion or XCO_2 retrieval because both have uncertainties. We similarly analysed time versus latitude distribution of surface CO_2 concentration difference with respect to ACTM simulation or CO_2^{ACTM} - $CO_2^{In\text{-}situ}$ considering accurate surface CO_2 concentration data from 53 measuring sites around the globe. Most of these sites are situated in the northern hemisphere having at least 90% data during study period (all sites geographical location can be visualised in Figure S7 in supporting information). MIROC4-ACTM simulated CO_2 near the surface is resampled to the nearest grid of surface sites (latitude, longitude, altitude) and measurement time from hourly interval model output. For each of the 53 sites, CO_2 concentration difference between ACTM and surface CO_2 concentration is calculated first, and then we linearly interpolate it spatially as presented in Figure 2(c). Results show no such annually and spatially systematic signature of CO_2 difference near the surface between equator to 45° S considering six stations (SEY: 4.7° S, ASC: 8° S, SMO: 14.2° S, NMB: 23.6° S, CPT: 34.4° S, CGO: 40.7° S) situated at different latitudes within this latitude band (Fig. S7). Considering the fact that inferred CO_2 difference may arise due to much lower data density for the in situ measurements within mentioned latitude bands, the analysis with the available sites suggests that systematic signatures of difference exist when we compared with OCO-2 XCO_2 (Fig. 2b). It hints at uncertainties in OCO-2 retrieval or systematic vertical transport error in the model (Schuh et al., 2019), given the relatively lower

https://doi.org/10.5194/egusphere-2024-3976
Preprint. Discussion started: 21 January 2025

uncertainty in in-situ CO_2 measurements compared to OCO-2 XCO_2. This vast part of the region remained challenging for a model to understand its error characteristics due to OCO-2 retrieval error. Further, we also compared the latitudinal average time series of CO_2 (XCO_2) difference of ACTM with surface (OCO-2) in Fig. 2(d). It shows an overall agreement of CO_2 difference with a correlation coefficient of 0.68 at 99% significance level with total time series variability (1-σ STDEV) of 0.28 and 0.19 ppm in CO_2 difference in surface as compared to OCO-2. Overall, this CO_2 space-time variability analysis clearly demonstrates that systematic signature in XCO_2 difference, primarily concentrated in southern mid and northern high latitudes, previous studies also indicated towards potential uncertainties may arise in retrieval over the ocean and or misrepresentation of vertical transport in inversion (Byrne et al., 2023; Frankenberg et al., 2016; Schuh et al., 2019). Since systematic errors in transport could result in inaccurate CO_2 flux estimates and, consequently, posterior simulated concentration (Deng et al., 2015; Stephens et al., 2007). In an inversion estimation, transport, surface CO_2 flux and CO_2 spatial gradient are closely interconnected so any misrepresentation in vertical or horizontal mixing consequently affects the estimated flux. This highlights the complexity of interpreting CO_2 differences across diverse regions, measurement platforms and error quantification of the optimised flux of inversions from surface and satellite measurements. Therefore, to better understand the consistency of CO_2 differences across different global regions and identify regions of major uncertainty which will enable us to address them effectively, we analysed CO_2 variation in different vertical tropospheric layers using vertical CO_2 profile datasets from aircraft measurements, discussed in section 3.2.

3.2 CO_2 difference in tropospheric layers

3.2.1 Over Globe

Figure 3 represents mean CO_2 difference or CO_2^{ACTM}-$CO_2^{aircraft}$ across different latitudes using individual aircraft observations for different tropospheric layers LT (light red), MT (orange), UT (dodger blue) and tropospheric Total Column (teal), color coded to represent different altitude ranges. Aircraft measurements are generally available in two modes: continuous measurements from the same site over a long period, and campaign measurements that cover extensive vertical and horizontal distances with high data density over a limited period. Therefore, we have subdivided aircraft measurements into two subcategories for our analysis: specific site aircrafts having latitude coverage maximum 5°(Fig. 3a) and campaign aircrafts having latitude coverage maximum 30° (Fig. 3b). Only those aircrafts having measurements during OCO-2 period are selected, each aircraft sampling location, number of data points at different latitude bins of 30° and altitude bins of 1000 meters is provided in the supplementary material (Fig. S8 and S9 gif for each aircraft category). Then, we calculated model-observation CO_2 difference for each aircraft measurement category. Therefore, estimated CO_2 difference serves as a model and observation mismatch for specific latitude (entire latitude range) for specific sites (campaign) aircraft with latitude information mentioned inside parenthesis of first x-axis tick marks in Fig. 3a (3b). Here, the second x-axis shows the number of data points in the corresponding aircraft campaign. Here, the number of data points or samples is critical when comparing CO_2 differences among aircraft. A higher number of samples provides better confidence to the calculated CO_2 difference while aircraft with fewer samples are considered less weightage.

https://doi.org/10.5194/egusphere-2024-3976
Preprint. Discussion started: 21 January 2025

Mean (variability) of CO_2 difference for LT, MT, UT and tropospheric column for specific sites aircraft are -0.45 (± 0.49), -0.32 (± 0.48), -0.34 (± 0.5), and -0.2 (± 0.41) respectively (Fig. 3a). It shows the highest mismatch in terms of mean exist in LT as compared to other tropospheric layers MT, UT and total tropospheric column, likely due to uncertainty in prior CO_2 flux or transport in LT. Studies have shown that in the LT, concentration changes are mainly regulated by surface CO_2 fluxes and diurnal-synoptic mixing patterns (Law et al., 2008; Patra et al., 2008). However, CO_2 change in UT is mainly dominated by changes in large scale dynamical transport, where surface emission has subdued influence. Hence, studies have found that coarse spatial resolution transport models adequately simulated CO_2 in the MT to UT regions (Baier et al., 2020; Niwa et al., 2011). Additionally, it is also noted that there is a systematic underestimation by the model in terms of magnitude in all tropospheric layers. Result shows minimum or maximum (near zero) model-observation CO_2 difference (ppm) observed for "esp" or "rta" (cma) aircraft at 49.48° N or 21.19° S (38.83° N) in the LT for specific sites aircraft. In the tropospheric column, maximum (minimum) CO_2 difference is observed in "cma" ("car") aircraft at 38.83° N (40.66° N) respectively. Further, it has been observed that the tropospheric column CO_2 difference matches pattern of CO_2 difference at LT at most aircraft sites; LT apparently contributes more to the total tropospheric column than MT and UT. Further, it could be seen that the overall mean model-observation CO_2 difference is highest in the northern mid-latitudes compared to the tropical latitudes of the northern and southern hemispheres.

Further, we have calculated XCO_2^{ACTM} - $XCO_2^{OCO\text{-}2}$ at those specific sites aircraft location considering 5°× 5° grid box surrounding it to check the difference similarity between XCO_2 and tropospheric column CO_2 selecting only specific times from OCO-2 of aircraft measurement. Results show XCO_2 difference mean (variability) of -0.37 (±0.38), highlighting that the model is underestimating and also has minimum variability as compared to any individual layers. On the other hand, CO_2 difference with campaign aircraft showed similar results; overall highest mean and variability exists in LT observed. Further, the overall mean (variability) of the tropospheric column is -0.39 (±0.1) controlled largely by CO_2 difference in LT. Here, we also check XCO_2 difference at those campaign aircraft considering their covered tracks and then taking the average of all XCO_2 differences to calculate a mean XCO_2 difference. Results show lesser variability in XCO_2 as compared to other layers and also negative mean XCO_2 represents overall underestimation by the model. It has been observed in both aircraft categories that the model has underestimated overall CO_2 concentration in all tropospheric layers and total columns, also the maximum mean and variability of CO_2 difference are in LT. These differences are attributed possibly due to underestimation by prior flux in the inversion or misrepresentation of transport in the model. To further investigate CO_2 differences altitude-wise, we considered individual vertical CO_2 profiles from different campaigns for different regions North America, Pacific, Southern Ocean, Atlantic, Amazon and Asia discussed in detail in subsequent sections.

3.2.2 North America, Pacific, Southern and Atlantic ocean

Figure 4(a) illustrates integrated tracks traversed by the aircraft during ATom campaign (ATom-1, ATom-2, ATom-3, ATom-4) across oceanic and land parts, subdivided into four segmented track categories corresponding to specific geographical regions delineated with different colours. Represented segments are North America and neighbours; east to west aircraft campaigning (magenta), Pacific; north to south aircraft campaigning (yellow), Southern Ocean; west to east aircraft campaigning (red), and Atlantic; south to north aircraft campaigning (green).

https://doi.org/10.5194/egusphere-2024-3976
Preprint. Discussion started: 21 January 2025

Figure 4(b) shows the mean XCO_2 difference taken considering a collocation criteria of 5° × 5° latitude-longitude grid box around sampling location and XCO_2 retrievals during corresponding ATom campaign period. We observed a maximum XCO_2 difference of nearly 2 ppm over 120° W and 90° W in North America and neighbouring land regions whereas oceanic regions, particularly Pacific and Atlantic are mostly confined within ±1 ppm at any specific latitude. We also checked the latitudinal bias MIROC4-ACTM against TCCON XCO_2 across the latitude during the ATom campaign period shown in Figure S11. This comparison also showed higher bias over this latitude location against TCCON sites at Park Falls, JPL, Lamont and East Trout Lake. Therefore, model bias is consistent both against OCO-2 and TCCON. Then, to understand the altitude-wise variation of CO_2^{ACTM} - $CO_2^{aircraft}$ difference at different tropospheric depths (LT, MT, UT, tropospheric column), we used ATom vertical CO_2 dataset. We also compared these CO_2 differences with OCO-2 across segmented ATom tracks (Fig. 4c-f). Result shows largest CO_2 difference in terms of mean ± STDEV (calculated taking 1-σ standard deviation) of CO_2 differences across longitude range is -0.41 ± 0.94 ppm exist in LT as compared to the other tropospheric layers likely due to uncertainty and large variability in prior land CO_2 flux near surface (Fig. 4c). When we compare CO_2 differences from other layers of different track segments, North America and neighbour's CO_2 difference at LT appears to be the highest, mainly occurring during the ATom-1 period (Figure S10). Moreover, OCO-2 XCO_2 difference also showed large variability with longitudinal mean CO_2 difference of -0.34 ± 1.07 ppm compared to aircraft tropospheric column CO_2 of -0.01 ± 0.48 ppm. This essentially reflects the model's overall good performance against ATom as compared to OCO-2 XCO_2. Similarly, ACTM and ATom CO_2 discrepancy was also evident in vertical cross-section, highest approximately ~ 2 ppm appeared at high latitude land regions during vegetation growing (respiration) period of northern hemisphere July-August, 2016 in ATom-1 (April-May, 2018 in ATom-4) (Figure S10). This large difference occurs across the vertical altitude range prominent above 8000 meters likely arises due to the coarse resolution of the ACTM model unable to represent the vertical transport. Needs further research on improving convective transport parameterization in forward model to improve vertical mixing (Patra et al., 2018). These results are also in line with the study Frankenberg et al., 2016. We have also validated model simulation with TCCON measurements during the ATom period, results also shown differences up to 1 ppm at the sites over northern America (Figure S11).

Other three segments of CO_2^{ACTM} - $CO_2^{aircraft}$ difference are primarily focused over oceanic regions (Southern, Pacific, Atlantic) where magnitude of ocean CO_2 flux variability is less as compared to land regions as much as 10 times less. Land and ocean CO_2 flux variability over the longitude and latitude band around ATom tracks for different campaigns is shown in Figure S12. Figure 4d shows that over the Southern Ocean, the model-observation CO_2 difference is lowest within ±0.2 ppm for each vertical tropospheric layer and 0.06 ppm for the aircraft tropospheric column, with minimal variability compared to other layers. When compared with other ATom segments, the Southern Ocean shows the lowest CO_2 difference in both mean and variability. This is because the aircraft sampling is at the background troposphere and is farthest from land having little influence from land CO_2 air mass. This reflects that the optimized MIROC4-ACTM model, considering 50 ground-based sites, simulates fairly well the aircraft background concentrations, however, it is unable to match a similar level of reproducibility for OCO-2 XCO_2. Further, the latitudinal CO_2 difference variability against the aircraft tropospheric column (lowest 8 km) is 0.15, compared to 0.77 with OCO-2 XCO_2. In most latitudes, OCO-2 XCO_2 differences are larger than aircraft CO_2, indicating likely retrieval errors in OCO-2 given the lower uncertainty in aircraft CO_2

https://doi.org/10.5194/egusphere-2024-3976
Preprint. Discussion started: 21 January 2025

measurements. This XCO_2 difference with OCO-2 over the southern ocean is mainly during the ATom-2 period (Fig. S14); however large XCO_2 difference pixels near 50° W and 70° W are during ATom-3 (September-October 2017; Fig. S15). Previous studies reported that OCO-2 ocean glint retrieval over southern ocean has more residual biases while comparing against individual measurements (TCCON, In-situ, OCO-2 land) in top-down inversion (Byrne et al. 2023; O'Dell et al., 2018). In addition, this is also location of the southern hemisphere zone of stratosphere-troposphere exchange (STE) vary greatly spatiotemporally due to significant vertical mixing which strongly changes with season, less constrained by model transport, which may also result in an error in estimated posterior concentration. Next, we analysed CO_2 differences over the southbound Pacific segments of the ATom campaign (Fig. 4e), it shows latitudinal CO_2 difference mean (variability) is highest of about -0.16 (± 0.53) ppm in LT, compared to MT and UT. On the other hand, aircraft tropospheric columns showed a mean (variability) difference of approximately -0.04 (± 0.38) ppm whereas OCO-2 XCO_2 with a value of 0.27 (± 0.42) ppm. This shows although the mean is significantly different however the variability in both CO_2 differences is close to each other, this is reflected in overall matching of both aircraft columns and OCO-2 XCO_2 (Fig. 4e). Lastly, we analysed CO_2 difference over the Atlantic i.e., longest northbound part of ATom campaign shown in Figure 4(f). Aircraft tropospheric column CO_2 difference of aircraft shows value of 0.03 ppm as compared to XCO_2 difference with OCO-2 showing value of 0.26 ppm. Although, it has been observed that the latitudinal CO_2 difference in the aircraft tropospheric column closely matches pattern in OCO-2 XCO_2. Another important point is that overall CO_2 differences variability in the Atlantic is observed higher as compared to the pacific segment especially over tropics within 30° S–30° N, more in-situ aircraft measurements are required to better understand the underlying error. Individual ATom campaigns results are presented in supplementary Figure S13-16.

3.2.3 Amazon

The climate-sensitive global tropic is a crucial part of the global carbon cycle due to the threats posed by climate change, especially the Amazon region, which holds the largest above-ground biomass (AGB) pool of approximately 123 ± PgC (Malhi et al., 2006; Santoro et al., 2010). Inversion based estimate showed Amazon was a carbon source of 0.3 ± 0.2 PgC/yr in agreement with bottom-up calculation (Alden et al., 2016; Beienen et al., 2015; Gatti et al., 2014, 2021a,c) during 2010-2019, though significant uncertainty remain. This is also the region under-sampled by OCO-2 retrievals due to clouds and high spatial resolution satellite monitoring is needed in the future (Frankenberg et al., 2024). Prevalent uncertainty in flux estimation in modelling approach and low sampling of satellites highlight the need for more research in understanding error better way and improving both inversion and retrievals methods over Amazon. In section 3.1, we observed large model-observation XCO_2 differences exist over South America, especially over Amazon. To investigate it further, we have utilised the vertical profile (VP) of CO_2 measurements from vertical aircraft campaigns across Brazilian Amazon sites, SAN, ALF, RBA, and TEF presented in Figure 5(a). The aircraft measurement has an accuracy of ~0.03 ppm (Gatti et al., 2023) and a detailed description of measurements can be found in Gatti et al., 2021a. Studies have shown that although these VPs are taken up to an altitude range of 4 km, they provide important insights into CO_2 variability near the surface (Gatti et al., 2023; Tejada et al., 2023). An important point to note here, since Amazon aircraft campaigns measure VPs of CO_2 approximately at an altitude up to 4 km, therefore, we considered the tropospheric column as 0 to 4 km and only those VPs having measurements at least 4 km are chosen for calculation. We kept

https://doi.org/10.5194/egusphere-2024-3976
Preprint. Discussion started: 21 January 2025

the same criteria for the data availability of 80% vertical bin filter for 500-meter bin resolution as mentioned previously in the methodology section.

Before analysing the ACTM bias against the Amazon aircraft CO_2, we validated ACTM simulated CO_2 with the aircraft CO_2 at these sites which are not used in the inversion, showing a good correlation (r) of ~0.8 at 95% significance level shown in Figure S17. We also checked that model able to capture TCCON XCO_2 at Manaus, Brazil with time series XCO_2 difference mean of 0.05 ppm, but the model shows higher differences (-1 ppm) with OCO-2 XCO_2 in Figure 2. It hints, OCO-2 retrieval likely have error could arise from Amazon dense vegetation cover, cloud cover-aerosols and high humid conditions which can block sunlight spectra, reduce the signal strength, limit valid sampling and increase retrieval error (Frankenberg et al., 2024; Taylor et al., 2016; Yu et al, 2019). These retrieval challenges precludes robust understanding of inversion error across the broader Amazonian region. To further check this error altitude wise, a monthly mean time series of ACTM-aircraft CO_2 difference considering all vertical profiles within a month is calculated for three vertical tropospheric layers, LT (lowest–2 km), MT (2–4 km) and tropospheric column (lowest-4 km) during OCO-2 measurement periods is presented in Figure 5c-f. Figure 5c represents CO_2 difference at SAN aircraft campaign sites having data gaps from mid-2015 to early-2017 because of no measurements conducted during this period. Maximum model-observation differences in terms of mean(variability) of 0.93(± 3.36) ppm observed in LT as compared to MT and tropospheric column. This mismatch is comparable with previous study by Basso et al. 2023. Further, OCO-2 XCO_2 difference showed overall negative mean of -0.83 ppm with variability of ± 1.04 ppm as compared to aircraft VPs profile with aircraft tropospheric column shown better constrained having value of 0.76 ppm. Further, we analysed VPs at the ALF site presented in Figure 5(d) shows overall that aircraft model-observation CO_2 difference matches well with XCO_2. CO_2 differences at LT, MT, tropospheric column, XCO_2 shows mean (STDEV) are -0.9 (± 4.24), 0.08 (± 2.03), -0.13 (± 2.48), -0.65 (± 1.03) respectively. Basso et al. 2023 has shown that some of this difference between inversion and aircraft CO_2 could be significantly improved (57% below 1.5 km and 49% above 3.5 km) when using regional aircraft CO_2 data in the inversions. . In RBA, CO_2 difference at LT, MT, tropospheric column, XCO_2 shows mean (STDEV) are -0.61 (± 4.33), -0.03 (± 2.52), 0.27 (± 2.95), -0.69 (± 1.04) respectively shown in Figure 5e. Therefore, it shows CO_2 difference with the aircraft tropospheric column (OCO-2 XCO_2) has opposite signature; it represents ACTM over (under) estimates considering the whole time window. In TEF, CO_2 difference at LT, MT, tropospheric column, XCO_2 shows mean (STDEV) are -0.4 (± 4.29), 0.64 (± 3.02), 0.19 (± 2.89), -1.37 (± 0.99) respectively presented in Figure 5f. Except for SAN, at all other sites, we observed that the ACTM matches in total column better with aircraft than OCO-2, and but this profile is still insufficient to match with XCO_2 needs further high profile measurement over this location. It is worth noting that the large discrepancy or bias in LT in RBA, TEF (SAN, ALF) during January-March (August-December) in west-central (south-east) Amazon regions may potentially arise due to fire CO_2 emission is reported in Basso et al. 2023. Since our inverse simulations using CASA biospheric flux lack observation-based biomass burning data, this could also affect the overall simulated concentration as well. We also checked monthly land CO_2 flux anomaly, calculated by taking area mean around campaign sites within 5° × 5° degree and then removing seasonal cycle from actual time series. We noticed no such anomalous flux change during the anomalous CO_2 difference period, likely due to the coarse resolution of the MIROC4-ACTM and also because no regional CO_2 data from Amazon is used in our inversion which could potentially capture Amazon land CO_2 flux changes better way (Fig. 5b; Fig. S1). Basso et al. 2023

https://doi.org/10.5194/egusphere-2024-3976
Preprint. Discussion started: 21 January 2025

highlighted the importance of assimilating Amazon aircraft measurements in deriving regional land CO_2 flux. In all Amazon aircraft sites, an increase in land CO_2 flux during 2015-16 was observed due to strong ENSO events occurred during this period also reported in Das et al. (2022).

3.2.4 Asia

In Asia there are very few aircraft campaigns for CO_2 measurements compared to Northern America and Europe (Crevoisiera et al., 2010; Xueref-Remy et al., 2011). Although, efforts have been made to measure CO_2 vertical profile over monsoon-dominated Indian subcontinents for a shorter time period (Vogel et al., 2023). Therefore, available long-term CO_2 measurements like CONTRAIL is very important to provide unprecedented insights into long-term CO_2 variability in UT/LS and model evaluations over these regions (Bisht et al., 2021; Das et al., 2022; Niwa et al., 2011). Therefore, we have utilised these measurements to compare and understand model-observations CO_2 difference for OCO-2 and CONTRAIL aircraft in different regions across Asia. Figure 6a depicts the spatial distribution of the CONTRAIL campaign CO_2 sampling location from January 2015-December, 2021, covering altitudes ranging up to ~12 to 14 km with topographic altitudes information (topography elevation data is downloaded from https://www.ncei.noaa.gov/products/etopo-global-relief-model). Here, we have selected four separate regions around airport locations delineated through deep green colors having CO_2 vertical profiles resulting from aircraft ascent or descent near airports. The four regions are namely Far East Asia, Southeast China, northern Southeast Asia and Equatorial Southeast Asia, based on the locations of airports. In Far East Asia, two airports are considered: Tokyo International Airport, Japan (site code: HND) (35.6° N, 139.8° E) and Narita International Airport (site code: NRT) (35.8° N, 140.4° E) are considered together, named TYO (35.7° N, 140.8° E); in Southeast China, Hong Kong International Airport (site code: HKG) (22.2° N, 113.6° E); in northern Southeast Asia, Suvarnabhumi International Airport, Thailand (site code: BKK) (13.7° N, 100.7° E); and in southern Southeast Asia, Singapore Changi International Airport, Singapore (site code: SIN) (1.4° N, 104.0° E), all airports are marked with a small square box in Figure 6a ,b. During the aforementioned period, no vertical sampling was performed over the Indian subcontinent and other two airports highlighted on map Incheon International Airport (site code: ICN) and Shanghai Pudong International Airport (site code: PVG), were not considered due to less number of sampling dataset. Figure 6b presents mean model-OCO-2 XCO_2 differences over sampling locations of CONTRAIL, showing mainly negative CO_2 difference ranging -0.5 to -1 ppm over boxed airports location highlighting likely reason is underestimation overall fossil emission of urban CO_2 signature in the model. There is very limited TCCON sites over city scale that validates OCO-2 XCO_2, however, Rißmann et al. (2022) using Munich Urban Carbon Column network (MUCCnet) XCO_2 across three sites over Germany found out OCO-2 has a RMSE of 0.6 ppm in urban site. Since OCO-2 has retrieval error over city scale it makes it challenging to discuss the sources of error could come from the model.

To understand this we analysed more robust CONTRAIL aircraft CO_2 (~0.2 ppm for each CONTRAIL data point), figure 6c-f represents a time series of model-observation CO_2 differences over each airport for different vertical depths of troposphere and XCO_2. Here, we have considered all CO_2 vertical profiles, selecting aircraft ascent and descent flight modes over airports within a month and done a monthly average for 200-meter vertical bins to calculate partial column CO_2 for aircraft and similarly for model simulations resampled at aircraft measurement location considering methodology described in section 2.4. For OCO-2, we computed the mean over designated

https://doi.org/10.5194/egusphere-2024-3976
Preprint. Discussion started: 21 January 2025

airports to calculate model-observation difference for XCO_2 for the specific months. Results show in far east Asia, TYO location CO_2 difference in LT, MT, UT, tropospheric column, XCO_2 shows mean of -2.0, -0.88, -0.73, -1.02, and -0.3 respectively. In HKG airport, the number of samples in LT was very less therefore ignored in the analysis however CO_2 difference in MT, UT, tropospheric column, XCO_2 shows values of -1.2, -0.99, -1.13 and -0.02 respectively. For northern Southeast Asia, BKK airport CO_2 difference at LT, MT, UT, tropospheric column, XCO_2 shows mean (STDEV) of -2.71 (± 1.67), -0.83 (± 0.74), -0.6 (± 0.59), -1.06 (± 0.71), and -0.1 (± 0.71) respectively. Further, in equatorial Southeast Asia, SIN airport difference at LT, MT, UT, tropospheric column, XCO_2 shows mean (STDEV) of -1.89 (± 1.26), -1.03 (± 0.54), -0.81 (± 0.59), -1.05 (± 0.56), and -0.25 (± 0.42) respectively.

Result indicates that in northern Southeast Asia and southern Southeast Asia, mean and variability of model-observation CO_2 difference is higher in LT as compared to UT, MT and weighs more. In all regions, model-observation difference for OCO-2 showed better constrained compared to aircraft measurements and readily observable that it closely matches the tropospheric column pattern. A notable fact in all regions is that the total time series mean of model-observation difference is negative for both aircraft (-1.02 to -1.13 ppm) and OCO-2 (-0.02 to -0.3 ppm), which would imply an underestimation of model simulated CO_2. While the OCO-2 XCO_2 vs MIROC4-ACTM differences are not statistically significant but the large and systematic CONTRAIL CO_2 vs MIROC4-ACTM differences may suggest that actual emission footprints captured by satellite observations are greater than the measurement resolution (~1.29 × 2.25 km^2 for OCO-2). It suggests OCO-2 capturing emissions from broader urban areas than its nominal resolution, possibly either due to the well-mixed nature of CO_2 and OCO-2 measuring total column or the spatial extent of urban footprint. Further, the large variability and significant differences between the aircraft CO_2 column and XCO_2 are evident in all regions. This is likely attributable to the selection of a specific box area, which surrounds airport locations situated in urban areas, one of the significant sources for fossil CO_2 emission. This inference is discussed in earlier studies (Patra et al., 2011; Umezawa et al. 2020), wherein they reported an urban emission footprint in CONTRAIL aircraft measurements conducted over airport megacities. The inversion process, utilized in this context, exclusively optimizes total CO_2 fluxes, for biosphere and ocean regions considering background sites, whereas this CONTRAIL measurement over airports having signature of urban interiors. Consequently, noteworthy disparities may emerge due to uncertainties associated with fossil fuel CO_2 emissions and also coarse horizontal resolution of MIROC4-ACTM (T42, ~2.8° × 2.8°) unable to reproduce the sub-grid-scale variations. This limitation does not influence optimized flux for the large area studies but affect our ability to simulate posterior concentrations, leading to underprediction of concentration near the surface over the emissions or sinks hotspots, e.g., anthropogenic emissions at the megacity areas or plumes of intense biomass burning. Note that the location of ascent and descent of the aircraft may change by seasons following the meteorological conditions, and thus the location of measurements less strictly follows year around. Previous studies underscore the critical role of fossil fuels in shaping simulated CO_2 dynamics, emphasizing their potential to introduce systematic errors in optimized surface fluxes (Suntharalingam et al., 2005; Wang et al., 2020).

3.3 Discussion and conclusions

https://doi.org/10.5194/egusphere-2024-3976
Preprint. Discussion started: 21 January 2025

The availability of the OCO-2, aircraft, and in-situ CO_2 observations, along with MIROC4-ACTM simulation at their corresponding measurement location and time, allows us with an opportunity to understand fine-scale CO_2 difference between the ACTM and OCO-2 more robustly. Because, this enables diagnosing CO_2 difference from near surface to different tropospheric layers, utilising surface, and aircraft observation to highlight persistent limitations in addressing inversion uncertainties.

- We demonstrated that MIROC4-ACTM, using only 50 surface-based CO_2 sites globally, accurately simulates tropospheric column and OCO-2 XCO_2, showing strong agreement with aircraft and TCCON data (correlation = 0.9, $p < 0.0001$) at most sampling sites.

- Our analysis highlighted that the regional hemispheric MIROC4-ACTM CO_2 difference with OCO-2 and in-situ measurements has heterogeneous signatures of CO_2 differences, particularly over land. However, Kulawik et al. 2019, noting that OCO-2 retrievals over lands have more random errors especially over Amazon which is less sampled by OCO-2 makes retrieval less reliable for comparison (Frankenberg et al., 2024). Additionally, comparison against in-situ indicates that OCO-2 likely has a systematic retrieval error over the southern hemisphere oceanic region. Both random error over land, less sampling of OCO-2 over global tropics and systematic error over ocean makes it difficult to detect and understand the uncertainties in inverse models in a global perspective. We need more vertical aircraft profile measurements to more robustly understand this error especially over the global tropics.

- Altitude wise comparison of CO_2 difference from categorical specific and campaign aircraft measurements around the globe consistently highlight the model's highest mismatch in LT as compared to MT, UT, and tropospheric columns. Additionally, LT contributes more to the mean and variability to the total tropospheric column than the MT, UT. This maximum uncertainty in the LT likely arises from the uncertainties in prior fluxes near the surface. In contrast, the MT and UT, where large-scale dynamical mixing predominates, show better model performance, likely due to realistic transport of the forward model. Further, aircraft tropospheric CO_2 columns are better reproduced by MIROC4-ACTM compared to individual tropospheric layers and OCO-2 XCO_2. Further, studies have shown OCO-2 XCO_2 is more prone to erroneous retrieval due to near surface aerosol and cloud contamination in LT which makes it challenging for total column comparison with model (Connor et al., 2016; Massie et al., 2021).

- Results from ATom show large CO_2 difference variability over North America regions as compared to other integrated tracks over ocean, likely because of the influence of land air mass having large variability in land CO_2 flux. Similarly, large CO_2 differences in aircraft sites over Amazon may likely arise due to uncertainty in prior flux and coarse resolution of the model unable to represent small scale variation requires more regional measurements in inversion, however, comparison against OCO-2 highlights robust requirement of good amount of valid retrievals to diagnose the inversion from large region perspective as well as insufficient high-altitude profile measurements (~4 km) demands more high profile measurements. Aircraft measurements over the remote background troposphere in the Pacific, Southern Ocean, and Atlantic showed the best match within 0.03 ppm when compared to OCO-2 with 0.2 ppm,

https://doi.org/10.5194/egusphere-2024-3976
Preprint. Discussion started: 21 January 2025

especially over the Southern Ocean. However, the model comparison with CONTRAIL has shown consistent more (less) underestimation against aircraft (OCO-2) CO_2 measurements for all airports in Asia. This discrepancy is likely due to the coarse resolution of the inversions unable to capture the signature of urban fossil CO_2 emissions and also for OCO-2 unable to capture the whole urban footprint.

Code availability

Data and figure processing codes prepared for this study will be made available upon reasonable request from the corresponding author. Inversion code used here is available on https://github.com/prabirp/co2l2r84.

Data availability

The ObsPack data product is available at https://gml.noaa.gov/ccgg/obspack/, CONTRAIL at https://www.cger.nies.go.jp/contrail/, Amazon aircraft campaign at https://doi.pangaea.de/10.1594/PANGAEA.926834. ACTM model outputs at aircraft sampling and OCO-2 sounding locations will be made accessible upon requests from corresponding authors.

Author contributions

CD, PKP and RKK developed the idea and methodology of the study. CD ran the entire analysis and prepared the main manuscript and supplementary. PKP, RKK and NC helped in review and editing. KI, and TM are part of the CONTRAIL CO_2 measurement group. All co-authors actively engaged in scientific discussions.

Competing interests

The authors declare that they have no conflict of interest.

Acknowledgments

All co-authors sincerely thanks to National Oceanic and Atmospheric Administration (NOAA), Japan Meteorological Agency (JMA), Commonwealth Scientific and Industrial Research Organisation (CSIRO), Laboratoire des sciences du climat et de l'environnement/Institut Pierre Simon Laplace (LSCE/IPSL), Scripps Institution of Oceanography (SIO), South African Weather Service (SAWS), Environment and Climate Change Canada (ECCC), Mt. Waliguan/ China Meteorological Administration (WLG/CMA), Tae-ahn Peninsula/Korean Meteorological Administration (TAP/KMA) for site observations, and the CONTRAIL, Amazon, ATom campaign teams for the aircraft observations. Surface in-situ CO_2 observations from Jungfraujoch are supported by the Swiss Federal Office for the Envrionment and ICOS Switzerland (ICOS-CH). This study would not have been possible without these CO_2 concentration measurements datasets around the globe.

Financial support

CD thanks to the Director of IIT Delhi, for providing PhD fellowship to carry out this work. This research is partly supported by the Environment Research and Technology Development Fund (JPMEERF24S12205) of the

https://doi.org/10.5194/egusphere-2024-3976
Preprint. Discussion started: 21 January 2025

Environmental Restoration and Conservation Agency of Japan, and the Arctic Challenge for Sustainability phase II (ArCS-II; JPMXD1420318865) Projects of the Ministry of Education, Culture, Sports, Science and Technology (MEXT).

Reference

Alden, C. B., Miller, J. B., Gatti, L. V., Gloor, M. M., Guan, K., Michalak, A. M., van der Laan-Luijkx, I. T., Touma, D., Andrews, A., Basso, L. S., Correia, C. S. C., Domingues, L. G., Joiner, J., Krol, M. C., Lyapustin, A. I., Peters, W., Shiga, Y. P., Thoning, K., van der Velde, I. R., … Diffenbaugh, N. S.: Regional atmospheric CO2 inversion reveals seasonal and geographic differences in Amazon net biome exchange. Global Change Biology, 22(10). https://doi.org/10.1111/gcb.13305, 2016.

Basso, L. S., Wilson, C., Chipperfield, M. P., Tejada, G., Cassol, H. L. G., Arai, E., Williams, M., Smallman, T. L., Peters, W., Naus, S., Miller, J. B., & Gloor, M.: Atmospheric CO_2 inversion reveals the Amazon as a minor carbon source caused by fire emissions, with forest uptake offsetting about half of these emissions. Atmospheric Chemistry and Physics, 23(17). https://doi.org/10.5194/acp-23-9685-2023, 2023.

Baier, B. C., Sweeney, C., Choi, Y., Davis, K. J., DiGangi, J. P., Feng, S., Fried, A., Halliday, H., Higgs, J., Lauvaux, T., Miller, B. R., Montzka, S. A., Newberger, T., Nowak, J. B., Patra, P., Richter, D., Walega, J., & Weibring, P.: Multispecies Assessment of Factors Influencing Regional CO_2 and CH_4 Enhancements During the Winter 2017 ACT-America Campaign. Journal of Geophysical Research: Atmospheres, 125(2). https://doi.org/10.1029/2019JD031339, 2020.

Bisht, J. S. H., Machida, T., Chandra, N., Tsuboi, K., Patra, P. K., Umezawa, T., Niwa, Y., Sawa, Y., Morimoto, S., Nakazawa, T., Saitoh, N., and Takigawa, M.: Seasonal variations of SF6, CO2, CH4, and N2O in the UT/LS region due to emissions, transport, and chemistry. Journal of Geophysical Research: Atmospheres, 126, e2020JD033541. https://doi.org/10.1029/2020JD033541, 2021.

Bovensmann, H., Burrows, J. P., Buchwitz, M., Frerick, J., Noël, S., Rozanov, V. V., Chance, K. V., & Goede, A. P. H.: SCIAMACHY: Mission objectives and measurement modes. Journal of the Atmospheric Sciences, 56(2). https://doi.org/10.1175/1520-0469(1999)056<0127:SMOAMM>2.0.CO;2, 1999.

Basu, S., Baker, D. F., Chevallier, F., Patra, P. K., Liu, J., and Miller, J. B.: The impact of transport model differences on CO2 surface flux estimates from OCO-2 retrievals of column average CO2, Atmos. Chem. Phys., 18, 7189–7215, https://doi.org/10.5194/acp-18-7189-2018, 2018.

Buchwitz, M., Reuter, M., Schneising, O., Hewson, W., Detmers, R. G., Boesch, H., Hasekamp, O. P., Aben, I., Bovensmann, H., Burrows, J. P., Butz, A., Chevallier, F., Dils, B., Frankenberg, C., Heymann, J., Lichtenberg, G., De Mazière, M., Notholt, J., Parker, R., … Wunch, D.: Global satellite observations of column-averaged carbon dioxide and methane: The GHG-CCI XCO_2 and XCH_4 CRDP3 data set. Remote Sensing of Environment, 203. https://doi.org/10.1016/j.rse.2016.12.027, 2017.

Byrne, B., Baker, D. F., Basu, S., Bertolacci, M., Bowman, K. W., Carroll, D., Chatterjee, A., Chevallier, F., Ciais, P., Cressie, N., Crisp, D., Crowell, S., Deng, F., Deng, Z., Deutscher, N. M., Dubey, M. K., Feng, S., García, O. E., Griffith, D. W. T., … Zeng, N.: National CO_2 budgets (2015-2020) inferred from atmospheric CO_2 observations in support of the global stocktake. *Earth System Science Data*, *15*(2), 963–1004. https://doi.org/10.5194/essd-15-963-2023, 2023.

Byrne, B., Jones, D. B. A., Strong, K., Zeng, Z. C., Deng, F., & Liu, J.: Sensitivity of CO_2 surface flux constraints to observational coverage. Journal of Geophysical Research, 122(12). https://doi.org/10.1002/2016JD026164, 2017.

Canadell, J.G., P.M.S. Monteiro, M.H. Costa, L. Cotrim da Cunha, P.M. Cox, A.V. Eliseev, S. Henson, M. Ishii, S. Jaccard, C. Koven, A. Lohila, P.K. Patra, S. Piao, J. Rogelj, S. Syampungani, S. Zaehle, and K. Zickfeld, 2021: Global Carbon and other Biogeochemical Cycles and Feedbacks. In Climate Change 2021: The Physical Science Basis. Contribution of Working Group I to the Sixth Assessment Report of the Intergovernmental Panel on Climate Change [Masson-Delmotte, V., P. Zhai, A. Pirani, S.L. Connors, C. Péan, S. Berger, N. Caud, Y. Chen, L. Goldfarb, M.I. Gomis, M. Huang, K. Leitzell, E. Lonnoy, J.B.R. Matthews, T.K. Maycock, T. Waterfield, O. Yelekçi, R. Yu, and B. Zhou (eds.)]. Cambridge University Press, Cambridge, United Kingdom and New York, NY, USA, pp. 673–816, doi: 10.1017/9781009157896.007, 2021

Chandra, N., Patra, P. K., Niwa, Y., Ito, A., Iida, Y., Goto, D., Morimoto, S., Kondo, M., Takigawa, M., Hajima, T., & Watanabe, M.: Estimated regional CO_2 flux and uncertainty based on an ensemble of atmospheric CO_2 inversions, Atmos. Chem. Phys., 22, 9215–9243, https://doi.org/10.5194/acp-22-9215-2022, 2022.

Chevallier, F., Ciais, P., Conway, T. J., Aalto, T., Anderson, B. E., Bousquet, P., Brunke, E. G., Ciattaglia, L., Esaki, Y., Fröhlich, M., Gomez, A., Gomez-Pelaez, A. J., Haszpra, L., Krummel, P. B., Langenfelds, R. L., Leuenberger, M., Machida, T., Maignan, F., Matsueda, H., … Worthy, D.: CO_2 surface fluxes at grid point

https://doi.org/10.5194/egusphere-2024-3976
Preprint. Discussion started: 21 January 2025

scale estimated from a global 21 year reanalysis of atmospheric measurements. Journal of Geophysical Research Atmospheres, 115(21). https://doi.org/10.1029/2010JD013887, 2010.

Chevallier, F., Deutscher, N. M., Conway, T. J., Ciais, P., Ciattaglia, L., Dohe, S., Fröhlich, M., Gomez-Pelaez, A. J., Griffith, D., Hase, F., Haszpra, L., Krummel, P., Kyrö, E., Labuschagne, C., Langenfelds, R., Machida, T., Maignan, F., Matsueda, H., Morino, I., Notholt, J., Ramonet, M., Sawa, Y., Schmidt, M., Sherlock, V., Steele, P., Strong, K., Sussmann, R., Wennberg, P., Wofsy, S., Worthy, D., Wunch, D., and Zimnoch, M.: Global CO_2 fluxes inferred from surface air-sample measurements and from TCCON retrievals of the CO_2 total column, Geophys. Res. Lett., 38, L24810, https://doi.org/10.1029/2011GL049899, 2011.

Chevallier, F., Palmer, P. I., Feng, L., Boesch, H., O'Dell, C. W., & Bousquet, P.: Toward robust and consistent regional CO_2 flux estimates from in situ and spaceborne measurements of atmospheric CO_2. Geophysical Research Letters, 41(3). https://doi.org/10.1002/2013GL058772, 2014.

Ciais, P., Rayner, P., Chevallier, F., Bousquet, P., Logan, M., Peylin, P., & Ramonet, M.: Atmospheric inversions for estimating CO_2 fluxes: Methods and perspectives. Climatic Change, 103(1–2). https://doi.org/10.1007/s10584-010-9909-3, 2010.

Connor, B., Bösch, H., McDuffie, J., Taylor, T., Fu, D., Frankenberg, C., O'Dell, C., Payne, V. H., Gunson, M., Pollock, R., Hobbs, J., Oyafuso, F., & Jiang, Y.: Quantification of uncertainties in OCO-2 measurements of XCO_2: Simulations and linear error analysis. Atmospheric Measurement Techniques, 9(10). https://doi.org/10.5194/amt-9-5227-2016, 2016.

Crevoisiera, C., Sweeney, C., Gloor, M., Sarmiento, J. L., & Tans, P. P.: Regional US carbon sinks from three-dimensional atmospheric CO_2 sampling. Proceedings of the National Academy of Sciences of the United States of America, 107(43). https://doi.org/10.1073/pnas.0900062107, 2010.

Crisp, D.: Measuring atmospheric carbon dioxide from space with the Orbiting Carbon Observatory-2 (OCO-2). Earth Observing Systems XX, 9607. https://doi.org/10.1117/12.2187291, 2015.

Crowell, S., Baker, D., Schuh, A., Basu, S., Jacobson, A. R., Chevallier, F., Liu, J., Deng, F., Feng, L., McKain, K., Chatterjee, A., Miller, J. B., Stephens, B. B., Eldering, A., Crisp, D., Schimel, D., Nassar, R., O'Dell, C. W., Oda, T., … Jones, D. B. A.: The 2015-2016 carbon cycle as seen from OCO-2 and the global in situ network. Atmospheric Chemistry and Physics, 19(15). https://doi.org/10.5194/acp-19-9797-2019, 2019.

Das, C., Kunchala, R. K., Chandra, N., Chhabra, A., & Pandya, M. R.: Characterizing the regional XCO2 variability and its association with ENSO over India inferred from GOSAT and OCO-2 satellite observations. Science of The Total Environment, 902, 166176. https://doi.org/10.1016/j.scitotenv.2023.166176, 2023.

Das, C., Kunchala, R. K., Chandra, N., Chmura, L., Nęcki, J., & Patra, P. K.: Meridional propagation of carbon dioxide (CO_2) growth rate and flux anomalies from the tropics due to ENSO. Geophysical Research Letters, 49, e2022GL100105. https://doi.org/10.1029/2022GL100105, 2022.

Deng, F., Jones, D. B. A., Walker, T. W., Keller, M., Bowman, K. W., Henze, D. K., Nassar, R., Kort, E. A., Wofsy, S. C., Walker, K. A., Bourassa, A. E., & Degenstein, D. A.: Sensitivity analysis of the potential impact of discrepancies in stratosphere-troposphere exchange on inferred sources and sinks of CO_2. Atmospheric Chemistry and Physics, 15(20). https://doi.org/10.5194/acp-15-11773-2015, 2015.

Eldering, A., O'Dell, C. W., Wennberg, P. O., Crisp, D., Gunson, M. R., Viatte, C., Avis, C., Braverman, A., Castano, R., Chang, A., Chapsky, L., Cheng, C., Connor, B., Dang, L., Doran, G., Fisher, B., Frankenberg, C., Fu, D., Granat, R., Hobbs, J., Lee, R. A. M., Mandrake, L., McDuffie, J., Miller, C. E., Myers, V., Natraj, V., O'Brien, D., Osterman, G. B., Oyafuso, F., Payne, V. H., Pollock, H. R., Polonsky, I., Roehl, C. M., Rosenberg, R., Schwandner, F., Smyth, M., Tang, V., Taylor, T. E., To, C., Wunch, D., and Yoshimizu, J.: The Orbiting Carbon Observatory-2: first 18 months of science data products, Atmos. 800 Meas. Tech., 10, 549–563, doi:10.5194/amt-10-549-2017, 2017.

Frankenberg, C., Bar-On, Y. M., Yin, Y., Wennberg, P. O., Jacob, D. J., & Michalak, A. M.: Data Drought in the Humid Tropics: How to Overcome the Cloud Barrier in Greenhouse Gas Remote Sensing. Geophysical Research Letters, 51(8). https://doi.org/10.1029/2024GL108791,2024.

Frankenberg, C., Kulawik, S. S., Wofsy, S. C., Chevallier, F., Daube, B., Kort, E. A., O'Dell, C., Olsen, E. T., & Osterman, G.: Using airborne HIAPER pole-to-pole observations (HIPPO) to evaluate model and remote sensing estimates of atmospheric carbon dioxide. Atmospheric Chemistry and Physics, 16(12). https://doi.org/10.5194/acp-16-7867-2016, 2016.

Friedlingstein, P., O'Sullivan, M., Jones, M. W., Andrew, R. M., Bakker, D. C. E., Hauck, J., Landschützer, P., Le Quéré, C., Luijkx, I. T., Peters, G. P., Peters, W., Pongratz, J., Schwingshackl, C., Sitch, S., Canadell, J. G., Ciais, P., Jackson, R. B., Alin, S. R., Anthoni, P., … Zheng, B.: Global Carbon Budget 2023. Earth System Science Data, 15(12). https://doi.org/10.5194/essd-15-5301-2023,2023.

Fu, Y., Liao, H., Tian, X. J., Gao, H., Jia, B., & Han, R.: Impact of Prior Terrestrial Carbon Fluxes on Simulations of Atmospheric CO_2 Concentrations. Journal of Geophysical Research: Atmospheres, 126(18). https://doi.org/10.1029/2021JD034794, 2021

https://doi.org/10.5194/egusphere-2024-3976
Preprint. Discussion started: 21 January 2025

Gatti, L. V., Basso, L. S., Miller, J. B., Gloor, M., Gatti Domingues, L., Cassol, H. L. G., Tejada, G., Aragão, L. E. O. C., Nobre, C., Peters, W., Marani, L., Arai, E., Sanches, A. H., Corrêa, S. M., Anderson, L., Von Randow, C., Correia, C. S. C., Crispim, S. P., & Neves, R. A. L.: Amazonia as a carbon source linked to deforestation and climate change. Nature, 595(7867). https://doi.org/10.1038/s41586-021-03629-6, 2021a.

Gatti, L.V., Correa, C.C.S., Domingues, L.G., Miller, J.B., Gloor, M., Martinewski, A., Basso, L.S., Santana, R., Crispim, S.P., Marani, L., Neves, R.L.: CO_2 Vertical Profiles on Four Sites over Amazon from 2010 to 2018. PANGAEA, https://doi.org/10.1594/PANGAEA.926834, 2021b.

Gatti, L. V., Cunha, C. L., Marani, L., Cassol, H. L. G., Messias, C. G., Arai, E., Denning, A. S., Soler, L. S., Almeida, C., Setzer, A., Domingues, L. G., Basso, L. S., Miller, J. B., Gloor, M., Correia, C. S. C., Tejada, G., Neves, R. A. L., Rajao, R., Nunes, F., … Machado, G. B. M.: Increased Amazon carbon emissions mainly from decline in law enforcement. Nature, 621(7978). https://doi.org/10.1038/s41586-023-06390-0, 2023.

Gatti, L. V., Gloor, M., Miller, J. B., Doughty, C. E., Malhi, Y., Domingues, L. G., Basso, L. S., Martinewski, A., Correia, C. S. C., Borges, V. F., Freitas, S., Braz, R., Anderson, L. O., Rocha, H., Grace, J., Phillips, O. L., & Lloyd, J.: Drought sensitivity of Amazonian carbon balance revealed by atmospheric measurements, Nature, 506, 76–80, https://doi.org/10.1038/nature12957, 2014.

Gatti, L. V, Melack, J., Basso, L. S., Restrepo-Coupe, N., Aguiar, A. P., Pangala, S., Saleska, S. R., Aragão, L. E. O., Phillips, O. L., & Armenteras, D.: Chapter 6A: The Amazon Carbon Budget. In Amazon Assessment Report 2021. https://doi.org/10.55161/vnbv7494, 2021c.

Inoue, M., Morino, I., Uchino, O., Miyamoto, Y., Yoshida, Y., Yokota, T., Machida, T., Sawa, Y., Matsueda, H., Sweeney, C., Tans, P. P., Andrews, A. E., Biraud, S. C., Tanaka, T., Kawakami, S., and Patra, P. K.: Validation of XCO2 de- rived from SWIR spectra of GOSAT TANSO-FTS with aircraft measurement data, Atmos. Chem. Phys., 13, 9771–9788, https://doi.org/10.5194/acp-13-9771-2013, 2013.

Ishijima, K., Machida, T., Niwa, Y., Tsuboi, K., Sawa, Y., Matsueda, H. & Sasakawa, M.: Atmospheric CO_2 mole fraction data of CONTRAIL-CME (most recent data), v2023.1.0, Center for Global Environmental Research, NIES, DOI:10.17595/20210827.001, (Reference date: 2023/08/13), 2021.

Jacobs, N., O'dell, C. W., Taylor, T. E., Logan, T. L., Byrne, B. K., Kiel, M., Kivi, R., Heikkinen, P., Merrelli, A., Payne, V. H., & Chatterjee, A.: The importance of digital elevation model accuracy in XCO_2 retrievals: improving the OCO-2 ACOS v11 product. https://doi.org/10.5194/amt-2023-151, 2023.

Keeling, C. D.: The Concentration and Isotopic Abundances of Carbon Dioxide in the Atmosphere. Tellus, 12(2), 200–203. https://doi.org/10.1111/j.2153-3490.1960.tb01300.x, 1960.

Kulawik, S. S., Crowell, S., Baker, D., Liu, J., McKain, K., Sweeney, C., Biraud, S. C., Wofsy, S., O'Dell, C. W., Wennberg, P. O., Wunch, D., Roehl, C. M., Deutscher, N. M., Kiel, M., Grif- fith, D. W. T., Velazco, V. A., Notholt, J., Warneke, T., Petri, C., De Mazière, M., Sha, M. K., Sussmann, R., Rettinger, M., Pollard, D. F., Morino, I., Uchino, O., Hase, F., Feist, D. G., Roche, S., Strong, K., Kivi, R., Iraci, L., Shiomi, K., Dubey, M. K., Sepulveda, E., Rodriguez, O. E. G., Té, Y., Jeseck, P., Heikkinen, P., Dlugokencky, E. J., Gunson, M. R., Elder- ing, A., Crisp, D., Fisher, B., and Osterman, G. B.: Characterization of OCO-2 and ACOS-GOSAT biases and errors for CO_2 flux estimates, Atmos. Meas. Tech. Discuss. [preprint], https://doi.org/10.5194/amt-2019-257, 2019.

Kuze, A., Suto, H., Nakajima, M., & Hamazaki, T.: Thermal and near infrared sensor for carbon observation Fourier-transform spectrometer on the Greenhouse Gases Observing Satellite for greenhouse gases monitoring. Applied Optics, 48(35). https://doi.org/10.1364/AO.48.00671, 2009.

Law, R. M., Peters, W., Rödenbeck, C., Aulagnier, C., Baker, I., Bergmann, D. J., Bousquet, P., Brandt, J., Bruhwiler, L., Cameron-Smith, P. J., Christensen, J. H., Delage, F., Denning, A. S., Fan, S., Geels, C., Houweling, S., Imasu, R., Karstens, U., Kawa, S. R., … Zhu, Z.: TransCom model simulations of hourly atmospheric CO2: Experimental overview and diurnal cycle results for 2002. *Global Biogeochemical Cycles*, *22*(3). https://doi.org/10.1029/2007GB003050, 2008.

Liang, A., Gong, W., Han, G., & Xiang, C. (2017). Comparison of satellite-observed XCO_2 from GOSAT, OCO-2, and ground-based TCCON. Remote Sensing, 9(10). https://doi.org/10.3390/rs9101033, 2017.

Taylor, T. E., O'Dell, C. W., Baker, D., Bruegge, C., Chang, A., Chapsky, L., Chatterjee, A., Cheng, C., Chevallier, F., Crisp, D., Dang, L., Drouin, B., Eldering, A., Feng, L., Fisher, B., Fu, D., Gunson, M., Haemmerle, V., Keller, G. R., … Zong, J.: Evaluating the consistency between OCO-2 and OCO-3 XCO_2 estimates derived from the NASA ACOS version 10 retrieval algorithm. Atmospheric Measurement Techniques, 16(12). https://doi.org/10.5194/amt-16-3173-2023,2023.

Taylor, T. E., O'Dell, C. W., Crisp, D., Kuze, A., Lindqvist, H., Wennberg, P. O., Chatterjee, A., Gunson, M., Eldering, A., Fisher, B., Kiel, M., Nelson, R. R., Merrelli, A., Osterman, G., Chevallier, F., Palmer, P. I., Feng, L., Deutscher, N. M., Dubey, M. K., … Wunch, D.: An 11-year record of XCO_2 estimates derived from GOSAT measurements using the NASA ACOS version 9 retrieval algorithm. Earth System Science Data, 14(1). https://doi.org/10.5194/essd-14-325-2022, 2022.

https://doi.org/10.5194/egusphere-2024-3976
Preprint. Discussion started: 21 January 2025

Tejada, G., Gatti, L. V., Basso, L. S., Cassol, H. L. G., Silva-Junior, C. H. L., Mataveli, G., Marani, L., Arai, E., Gloor, M., Miller, J. B., Cunha, C. L., Domingues, L. G., Ipia, A., Correia, C. S. C., Crispim, S. P., Neves, R. A. L., & Von Randow, C.: CO_2 emissions in the Amazon: are bottom-up estimates from land use and cover datasets consistent with top-down estimates based on atmospheric measurements? Frontiers in Forests and Global Change, 6. https://doi.org/10.3389/ffgc.2023.1107580, 2023.

Machida, T., Matsueda, H., Sawa, Y., Nakagawa, Y., Hirotani, K., Kondo, N., Goto, K., Nakazawa, T., Ishikawa, K., and Ogawa, T.:Worldwide measurements of atmospheric CO_2 and other trace gas species using commercial airlines. Journal of Atmospheric and Oceanic Technology, 25(10), 1744–1754. https://doi.org/10.1175/2008JTECHA1082.1, 2008.

Malhi, Y., Wood, D., Baker, T. R., Wright, J., Phillips, O. L., Cochrane, T., Meir, P., Chave, J., Almeida, S., Arroyo, L., Higuchi, N., Killeen, T. J., Laurance, S. G., Laurance, W. F., Lewis, S. L., Monteagudo, A., Neill, D. A., Vargas, P. N., Pitman, N. C. A., … Vinceti, B.: The regional variation of aboveground live biomass in old-growth Amazonian forests. Global Change Biology, 12(7). https://doi.org/10.1111/j.1365-2486.2006.01120.x, 2006.

Massie, S. T., Cronk, H., Merrelli, A., O'Dell, C., Sebastian Schmidt, K., Chen, H., & Baker, D.: Analysis of 3D cloud effects in OCO-2 XCO_2 retrievals. Atmospheric Measurement Techniques, 14(2). https://doi.org/10.5194/amt-14-1475-2021, 2021.

Matsueda, H., Machida, T., Sawa, Y., Nakagawa, Y., Hirotani, K., Ikeda, H., Kondo, N., and Goto, K.: Evaluation of atmospheric CO_2 measurements from new flask air sampling of JAL airliner observations. Papers in Meteorology and Geophysics, 59, 1–17. https://doi.org/10.2467/mripapers.59.1, 2008.

Mauceri, S., Massie, S., & Schmidt, S.: Correcting 3D cloud effects in XCO_2 retrievals from the Orbiting Carbon Observatory-2 (OCO-2). Atmospheric Measurement Techniques, 16(6). https://doi.org/10.5194/amt-16-1461-2023, 2023.

Merrelli, A., Bennartz, R., O'Dell, C. W., and Taylor, T. E.: Estimating bias in the OCO-2 retrieval algorithm caused by 3-D radiation scattering from unresolved boundary layer clouds, Atmos. Meas. Tech., 8, 1641–1656, https://doi.org/10.5194/amt-8-1641-2015, 2015.

Miller, C. E., Crisp, D., DeCola, P. L., Olsen, S. C., Randerson, J. T., Michalak, A. M., Alkhaled, A., Rayner, P., Jacob, D. J., Suntharalingam, P., Jones, D. B. A., Denning, A. S., Nicholls, M. E., Doney, S. C., Pawson, S., Boesch, H., Connor, B. J., Fung, I. Y., O'Brien, D., … Law, R. M.: Precision requirements for space-based XCO_2 data. Journal of Geophysical Research Atmospheres, 112(10). https://doi.org/10.1029/2006JD007659, 2007.

Müller, A., Tanimoto, H., Sugita, T., Machida, T., Nakaoka, S., Pa- tra, P. K., Laughner, J., and Crisp, D.: New approach to eval- uate satellite-derived XCO2 over oceans by integrating ship and aircraft observations, Atmos. Chem. Phys., 21, 8255–8271, https://doi.org/10.5194/acp-21-8255-2021, 2021.

Niwa, Y., Patra, P. K., Sawa, Y., Machida, T., Matsueda, H., Belikov, D., Maki, T., Ikegami, M., Imasu, R., Maksyutov, S., Oda, T., Satoh, M., & Takigawa, M.: Three-dimensional variations of atmospheric CO_2: Aircraft measurements and multi-transport model simulations. Atmospheric Chemistry and Physics, 11(24), 13359–13375. https://doi.org/10.5194/acp-11-13359-2011, 2011.

O'Dell, C. W., Eldering, A., Wennberg, P. O., Crisp, D., Gunson, M. R., Fisher, B., Frankenberg, C., Kiel, M., Lindqvist, H., Mandrake, L., Merrelli, A., Natraj, V., Nelson, R. R., Osterman, G. B., Payne, V. H., Taylor, T. E., Wunch, D., Drouin, B. J., Oyafuso, F., … Velazco, V. A.: Improved retrievals of carbon dioxide from Orbiting Carbon Observatory-2 with the version 8 ACOS algorithm. Atmospheric Measurement Techniques, 11(12). https://doi.org/10.5194/amt-11-6539-2018, 2018.

Patra, P.K., Crisp, D., Kaiser, J.W., Wunch, D., Saeki, T., Ichii, K., Sekiya, T., Wennberg, P.O., Feist, D.G., Pollard, D.F., Griffith, D.W.T., Velazco, V.A., De Maziere, M., Sha, M.K., Roehl, C., Chatterjee, A., Ishijima, K.: The Orbiting Carbon Observatory (OCO-2) tracks 2-3 peta-gram increase in carbon release to the atmosphere during the 2014-2016 El Nino. Sci. Rep. 7, 13567 https://doi.org/ 10.1038/s41598-017-13459-0, 2017.

Patra, P. K., Law, R. M., Peters, W., Rödenbeck, C., Takigawa, M., Aulagnier, C., Baker, I., Bergmann, D. J., Bousquet, P., Brandt, J., Bruhwiler, L., Cameron-Smith, P. J., Christensen, J. H., Delage, F., Denning, A. S., Fan, S., Geels, C., Houweling, S., Imasu, R., … Zhu, Z.: TransCom model simulations of hourly atmospheric CO2: Analysis of synoptic-scale variations for the period 2002-2003. *Global Biogeochemical Cycles*, *22*(4). https://doi.org/10.1029/2007GB003081, 2008.

Patra, P. K., Maksyutov, S., Sasano, Y., Nakajima, H., Inoue, G., & Nakazawa, T.: An evaluation of CO_2 observations with solar occultation FTS for inclined-orbit satellite sensor for surface source inversion. Journal of Geophysical Research: Atmospheres, 108(24). https://doi.org/10.1029/2003jd003661, 2003.

Patra, P. K., Niwa, Y., Schuck, T. J., Brenninkmeijer, C. A. M., Machida, T., Matsueda, H., & Sawa, Y.: Carbon balance of South Asia constrained by passenger aircraft CO_2 measurements. Atmospheric Chemistry and Physics, 11(9). https://doi.org/10.5194/acp-11-4163-2011, 2011.

https://doi.org/10.5194/egusphere-2024-3976
Preprint. Discussion started: 21 January 2025

Patra, P. K., Takigawa, M., Watanabe, S., Chandra, N., Ishi- jima, K., and Yamashita, Y.: Improved Chemical Tracer Simulation by MIROC4.0-based Atmospheric Chemistry- Transport Model (MIROC4-ACTM), SOLA, 14, 91–96, https://doi.org/10.2151/sola.2018-016, 2018.

Peylin, P., Law, R. M., Gurney, K. R., Chevallier, F., Jacobson, A. R., Maki, T., Niwa, Y., Patra, P. K., Peters, W., Rayner, P. J., Rödenbeck, C., Van Der Laan-Luijkx, I. T., & Zhang, X.: Global atmospheric carbon budget: Results from an ensemble of atmospheric CO_2 inversions. Biogeosciences, 10(10), 6699–6720. https://doi.org/10.5194/bg-10-6699-2013, 2013.

Philip, S., Johnson, M. S., Baker, D. F., Basu, S., Tiwari, Y. K., Indira, N. K., Ramonet, M., & Poulter, B.: OCO-2 Satellite-Imposed Constraints on Terrestrial Biospheric CO_2 Fluxes Over South Asia. Journal of Geophysical Research: Atmospheres, 127(3). https://doi.org/10.1029/2021JD035035, 2022.

Rastogi, B., Miller, J. B., Trudeau, M., Andrews, A. E., Hu, L., Mountain, M., Nehrkorn, T., Baier, B., McKain, K., Mund, J., Guan, K., & Alden, C. B.: Evaluating consistency between total column CO_2 retrievals from OCO-2 and the in situ network over North America: Implications for carbon flux estimation. Atmospheric Chemistry and Physics, 21(18). https://doi.org/10.5194/acp-21-14385-2021, 2021.

Rißmann, M., Chen, J., Osterman, G., Zhao, X., Dietrich, F., Makowski, M., Hase, F., and Kiel, M.: Comparison of OCO-2 target observations to MUCCnet – is it possible to capture urban XCO2 gradients from space?, Atmos. Meas. Tech., 15, 6605–6623, https://doi.org/10.5194/amt-15-6605-2022, 2022.

Santoro, M., Cartus, O., Carvalhais, N., Rozendaal, D. M. A., Avitabile, V., Araza, A., de Bruin, S., Herold, M., Quegan, S., Rodríguez-Veiga, P., Balzter, H., Carreiras, J., Schepaschenko, D., Korets, M., Shimada, M., Itoh, T., Moreno Martínez, Á., Cavlovic, J., Cazzolla Gatti, R., da Conceição Bispo, P., Dewnath, N., Labrière, N., Liang, J., Lindsell, J., Mitchard, E. T. A., Morel, A., Pacheco Pascagaza, A. M., Ryan, C. M., Slik, F., Vaglio Laurin, G., Verbeeck, H., Wijaya, A., and Willcock, S.: The global forest above-ground biomass pool for 2010 estimated from high-resolution satellite observations, Earth Syst. Sci. Data, 13, 3927–3950, https://doi.org/10.5194/essd-13-3927-2021, 2021.

Schimel, D., Pavlick, R., Fisher, J. B., Asner, G. P., Saatchi, S., Townsend, P., Miller, C., Frankenberg, C., Hibbard, K., & Cox, P.: Observing terrestrial ecosystems and the carbon cycle from space. In Global Change Biology (Vol. 21, Issue 5). https://doi.org/10.1111/gcb.12822, 2015.

Schuh, A. E., Jacobson, A. R., Basu, S., Weir, B., Baker, D., Bowman, K., Chevallier, F., Crowell, S., Davis, K. J., Deng, F., Denning, S., Feng, L., Jones, D., Liu, J., & Palmer, P. I.: Quantifying the Impact of Atmospheric Transport Uncertainty on CO_2 Surface Flux Estimates. Global Biogeochemical Cycles, 33(4). https://doi.org/10.1029/2018GB006086, 2019.

Schuldt, K.N., Mund, J., Luijkx, I.T., Aalto, T., Abshire, J.B., Aikin, K., Andrews, A., Aoki, S., Apadula, F., Baier, B., Bakwin, P., Bartyzel, J., Bentz, G., Bergamaschi, P., Beyersdorf, A., Biermann, T., Biraud, S.C., Boenisch, H., Bowling, D.,…, Bulk, P. v.: Multi-laboratory compilation of atmospheric carbon dioxide data for the period 1957-2021; obspack_co2_1_GLOBALVIEWplus_v8.0_2022-08-27. NOAA Global Monitoring Laboratory. http://doi.org/10.25925/20220808, 2022.

Stephens, B. B., Gurney, K. R., Tans, P. P., Sweeney, C., Peters, W., Bruhwiler, L., Ciais, P., Ramonet, M., Bousquet, P., Nakazawa, T., Aoki, S., Machida, T., Inoue, G., Vinnichenko, N., Lloyd, J., Jordan, A., Heimann, M., Shibistova, O., Langenfelds, R. L., … Denning, A. S.: Weak northern and strong tropical land carbon uptake from vertical profiles of atmospheric CO2. Science, 316(5832). https://doi.org/10.1126/science.1137004, 2007.

Suntharalingam, P., Randerson, J. T., Krakauer, N., Logan, J. A., & Jacob, D. J.: Influence of reduced carbon emissions and oxidation on the distribution of atmospheric CO_2: Implications for inversion analyses. Global Biogeochemical Cycles, 19(4). https://doi.org/10.1029/2005GB002466, 2005.

Thoning, K. W., Tans, P. P., & Komhyr, W. D.: Atmospheric Carbon Dioxide at Mauna Loa Observatory 2. Analysis of the NOAA GMCC Data, 1974-1985. In JOURNAL OF GEOPHYSICAL RESEARCH (Vol. 94, Issue D6), 1989.

Umezawa, T., Matsueda, H., Oda, T., Higuchi, K., Sawa, Y., Machida, T., Niwa, Y., & Maksyutov, S.: Statistical characterization of urban CO2 emission signals observed by commercial airliner measurements. Scientific Reports, 10(1). https://doi.org/10.1038/s41598-020-64769-9, 2020.

Villalobos, Y., Rayner, P., Thomas, S., & Silver, J.: The potential of Orbiting Carbon Observatory-2 data to reduce the uncertainties in CO_2 surface fluxes over Australia using a variational assimilation scheme. Atmospheric Chemistry and Physics, 20(14). https://doi.org/10.5194/acp-20-8473-2020, 2020.

Vogel, B., Volk, C. M., Wintel, J., Lauther, V., Müller, R., Patra, P. K., Riese, M., Terao, Y., & Stroh, F.: Reconstructing high-resolution in-situ vertical carbon dioxide profiles in the sparsely monitored Asian monsoon region. Communications Earth and Environment, 4(1). https://doi.org/10.1038/s43247-023-00725-5, 2023.

Wang, J. S., Oda, T., Kawa, S. R., Strode, S. A., Baker, D. F., Ott, L. E., & Pawson, S.: The impacts of fossil fuel emission uncertainties and accounting for 3-D chemical CO_2 production on inverse natural carbon flux

https://doi.org/10.5194/egusphere-2024-3976
Preprint. Discussion started: 21 January 2025

estimates from satellite and in situ data. Environmental Research Letters, 15(8). https://doi.org/10.1088/1748-9326/ab9795 , 2020.

WDCGG (World Data Centre for Greenhouse Gases): World Data Centre (WDC) operated by the Japan Meteorological Agency (JMA) under the Global Atmosphere Watch (GAW) programme of the World Meteorological Organization (WMO) [data set], https://gaw.kishou.go.jp/

Wofsy, S. C.: HIAPER Pole-to-Pole Observations (HIPPO): fine- grained, global-scale measurements of climatically important atmospheric gases and aerosols, Philos. T. R. Soc. A., 369, 2073– 2086, https://doi.org/10.1098/rsta.2010.0313, 2011.

Wofsy, S.C., S. Afshar, H.M. Allen, E.C. Apel, E.C. Asher, B. Barletta, J. Bent, H. Bian, B.C. Biggs, D.R. Blake, N. Blake, I. Bourgeois, C.A. Brock, W.H. Brune, J.W. Budney, T.P. Bui, A. Butler, P. Campuzano-Jost, C.S. Chang, M. Chin, R. Commane, G. Correa, J.D. Crounse, P. D. Cullis, B.C. Daube, D.A. Day, J.M. Dean-Day, J.E. Dibb, J.P. DiGangi, G.S. Diskin, M. Dollner, J.W. Elkins, F. Erdesz, A.M. Fiore, C.M. Flynn, K.D. Froyd, D.W. Gesler, S.R. Hall, T.F. Hanisco, R.A. Hannun, A.J. Hills, E.J. Hintsa, A. Hoffman, R.S. Hornbrook, L.G. Huey, S. Hughes, J.L. Jimenez, B.J. Johnson, J.M. Katich, R.F. Keeling, M.J. Kim, A. Kupc, L.R. Lait, K. McKain, R.J. Mclaughlin, S. Meinardi, D.O. Miller, S.A. Montzka, F.L. Moore, E.J. Morgan, D.M. Murphy, L.T. Murray, B.A. Nault, J.A. Neuman, P.A. Newman, J.M. Nicely, X. Pan, W. Paplawsky, J. Peischl, M.J. Prather, D.J. Price, E.A. Ray, J.M. Reeves, M. Richardson, A.W. Rollins, K.H. Rosenlof, T.B. Ryerson, E. Scheuer, G.P. Schill, J.C. Schroder, J.P. Schwarz, J.M. St.Clair, S.D. Steenrod, B.B. Stephens, S.A. Strode, C. Sweeney, D. Tanner, A.P. Teng, A.B. Thames, C.R. Thompson, K. Ullmann, P.R. Veres, N.L. Wagner, A. Watt, R. Weber, B.B. Weinzierl, P.O. Wennberg, C.J. Williamson, J.C. Wilson, G.M. Wolfe, C.T. Woods, L.H. Zeng, and N. Vieznor.: ATom: Merged Atmospheric Chemistry, Trace Gases, and Aerosols, Version 2. ORNL DAAC, Oak Ridge, Tennessee, USA. https://doi.org/10.3334/ORNLDAAC/1925, 2021.

Wunch, D., Wennberg, P. O., Osterman, G., Fisher, B., Naylor, B., Roehl, M. C., O'Dell, C., Mandrake, L., Viatte, C., Kiel, M., Griffith, D. W. T., Deutscher, N. M., Velazco, V. A., Notholt, J., Warneke, T., Petri, C., De Maziere, M., Sha, M. K., Sussmann, R., … Eldering, A. (2017). Comparisons of the Orbiting Carbon Observatory-2 (OCO-2) XCO_2 measurements with TCCON. In Atmospheric Measurement Techniques (Vol. 10, Issue 6). https://doi.org/10.5194/amt-10-2209-2017, 2017.

Xueref-Remy, I., Bousquet, P., Carouge, C., Rivier, L., & Ciais, P.: Variability and budget of CO_2 in Europe: Analysis of the CAATER airborne campaigns-Part 2: Comparison of CO_2 vertical variability and fluxes between observations and a odelling framework. Atmospheric Chemistry and Physics, 11(12). https://doi.org/10.5194/acp-11-5673-2011, 2011.

Yu, L., Wen, J., Chang, C. Y., Frankenberg, C., & Sun, Y.: High-Resolution Global Contiguous SIF of OCO-2. *Geophysical Research Letters*, 46, 1449–1458. https://doi.org/10.1029/2018GL081109, 2019.

https://doi.org/10.5194/egusphere-2024-3976
Preprint. Discussion started: 21 January 2025

Figures

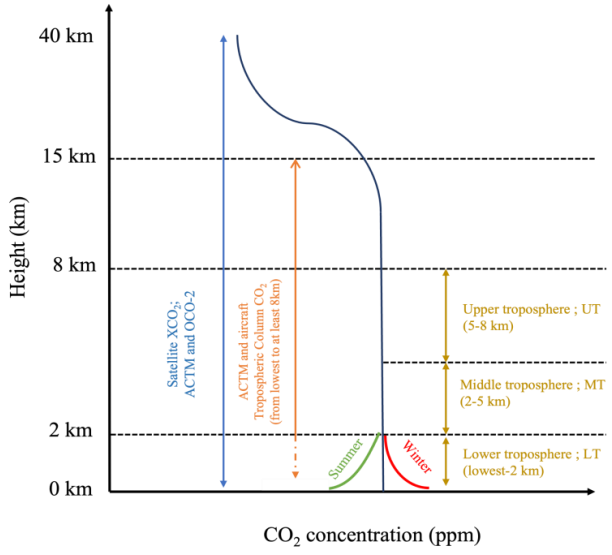

Figure 1: Schematic of CO_2 concentration vertical profile (dark blue line) by satellite, ACTM, and aircraft CO_2 (orange, golden) Arrowheads represent different layers of the atmosphere, specifically LT (lowest–2 km), MT (2–5 km), UT (5–8 km), and the tropospheric column (lowest–8 km) corresponds to the aircraft CO_2 measurement. Blue arrow represents total variation captured by satellite covers from surface to top of the atmosphere.

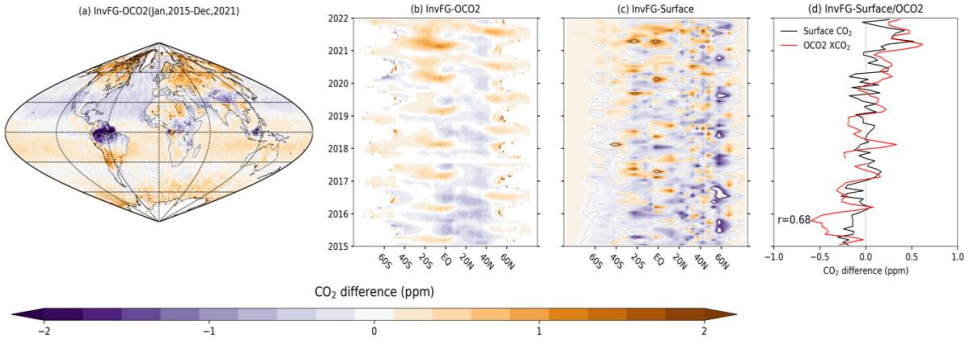

Figure 2: CO_2 space-time variability with (a) spatial mean XCO_2 difference map between InvFG and OCO-2 during January,2015-December,2021. (b) Time vs latitude distribution of XCO_2 difference between InvFG and OCO-2 considering mean across global longitude. (c) Time vs latitude cross-section of CO_2 concentration difference between InvFG and in-situ CO_2 measurement, considering CO_2 from 53 surface sites. (d) Latitude

https://doi.org/10.5194/egusphere-2024-3976
Preprint. Discussion started: 21 January 2025

996 averaged time series of CO_2 (XCO_2) concentration difference between InvFG and Surface (OCO-2) respectively
997 represented by black (red) colours. "r" value in panel-d represents correlation between time series of surface and
998 OCO-2 difference at 99% significance level.
999
1000

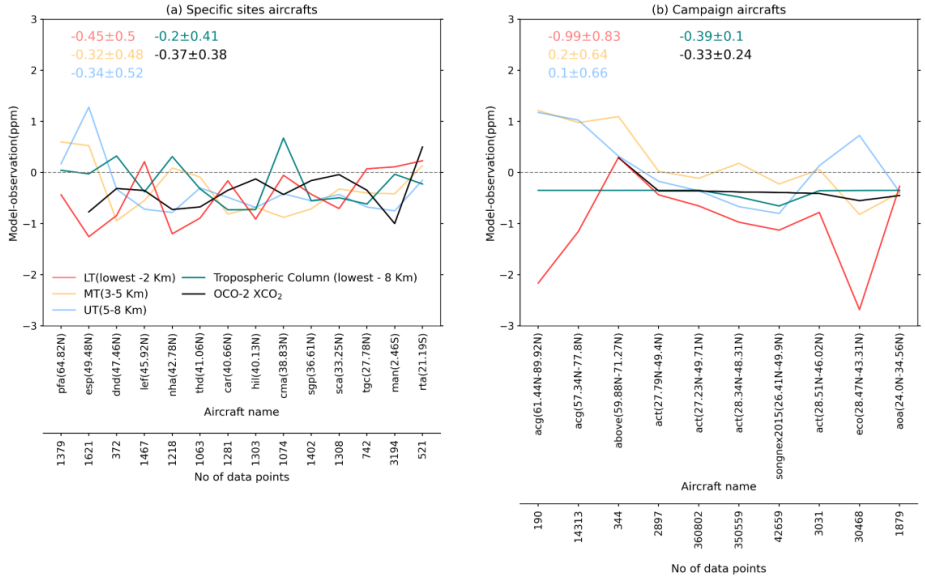

1001
1002
1003 **Figure 3.** Mean model-observation CO_2 difference (ppm) at different vertical tropospheric depths LT (light red),
1004 MT (orange), UT (dodger blue), total column (teal) and XCO_2 for specific sites aircraft (panel–a) and campaign
1005 aircraft measurements having latitudinal coverage maximum 30° (panel–b). Aircrafts names are organized based
1006 on aircraft observations location, progressing from high latitudes in the Northern Hemisphere, through the equator,
1007 to southern latitudes. The second x-axis represents a number of data points for specific aircraft observation. The
1008 first and second number inside the panel represents mean and 1-σ standard deviation (STDEV) of model-
1009 observation difference across latitude for each tropospheric layer.
1010

https://doi.org/10.5194/egusphere-2024-3976
Preprint. Discussion started: 21 January 2025

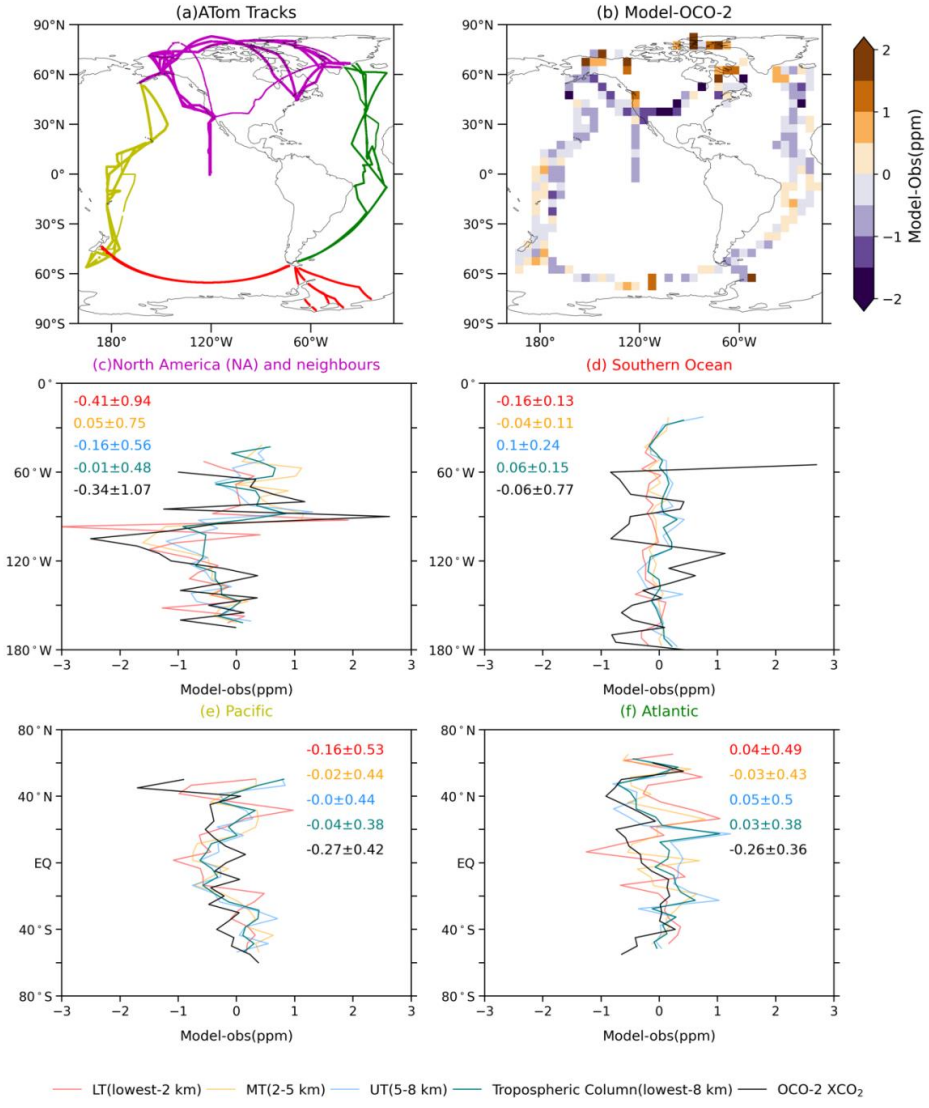

Figure 4: (a) Integrated tracks traversed during ATom campaigns (ATom-1, ATom-2, ATom-3 and ATom-4). (b) Spatial model-observation XCO_2 difference against OCO-2 over ATom integrated track during campaign (c), (d), (e), and (f) shows model-observation CO_2 difference over different tropospheric layers from vertical CO_2 profile measurements of ATom and XCO_2 from OCO-2 for North America and neighbours, Southern Ocean, Pacific, and Atlantic segments respectively. Tropospheric layers are LT (light red), MT (orange), UT (dodger blue) and Total Column (teal), and OCO-2 XCO_2 (black) representation for difference against OCO-2. The first and second number on the right side of each middle and bottom panel represents the mean and 1-σ standard deviation (STDEV) of model-observation difference across latitude or longitude, respectively.

https://doi.org/10.5194/egusphere-2024-3976
Preprint. Discussion started: 21 January 2025

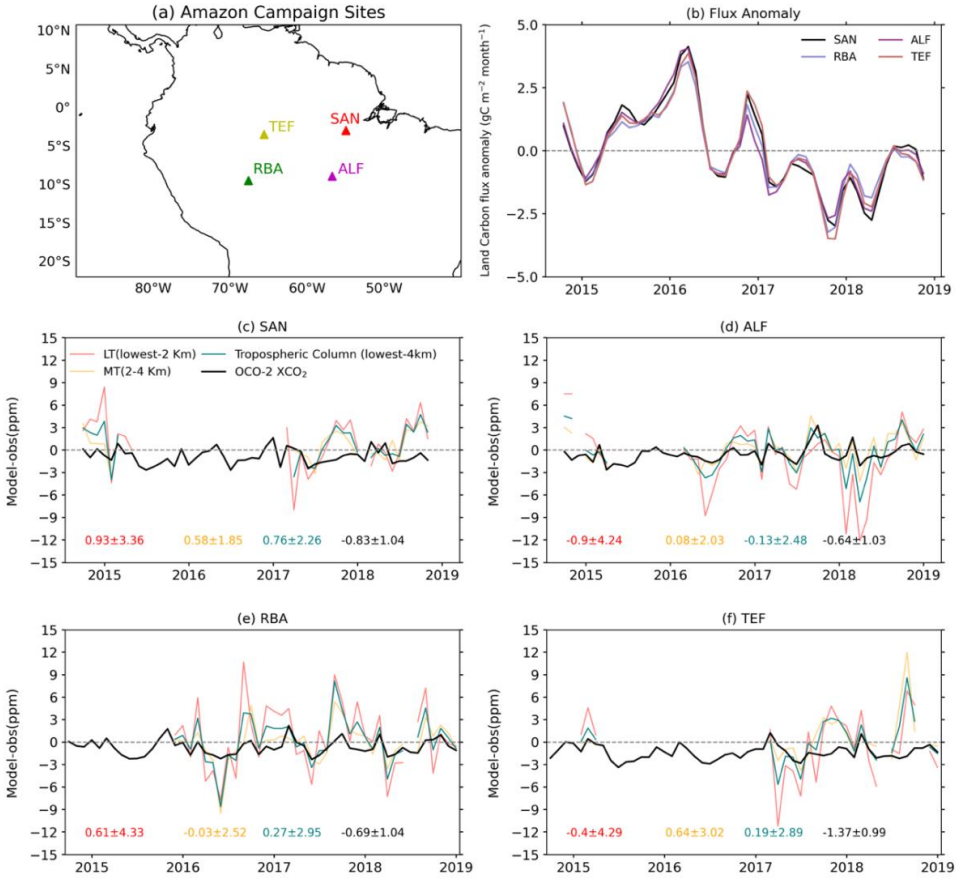

Figure 5: (a) Amazon aircraft vertical CO_2 profile campaign sites, SAN, ALF, RBA, and TEF. (b) Time series of land carbon flux anomalies at the campaign sites. (c), (d), (e) and (f) represent a time series of model-observation CO_2 differences for LT, MT, and tropospheric column, and XCO_2 during OCO-2 measurement periods for SAN, ALF, RBA and TEF, respectively. The numbers inside the middle and bottom panels represent the mean and 1-σ standard deviation (STDEV) of model-observation CO_2 difference over the time period.

https://doi.org/10.5194/egusphere-2024-3976
Preprint. Discussion started: 21 January 2025

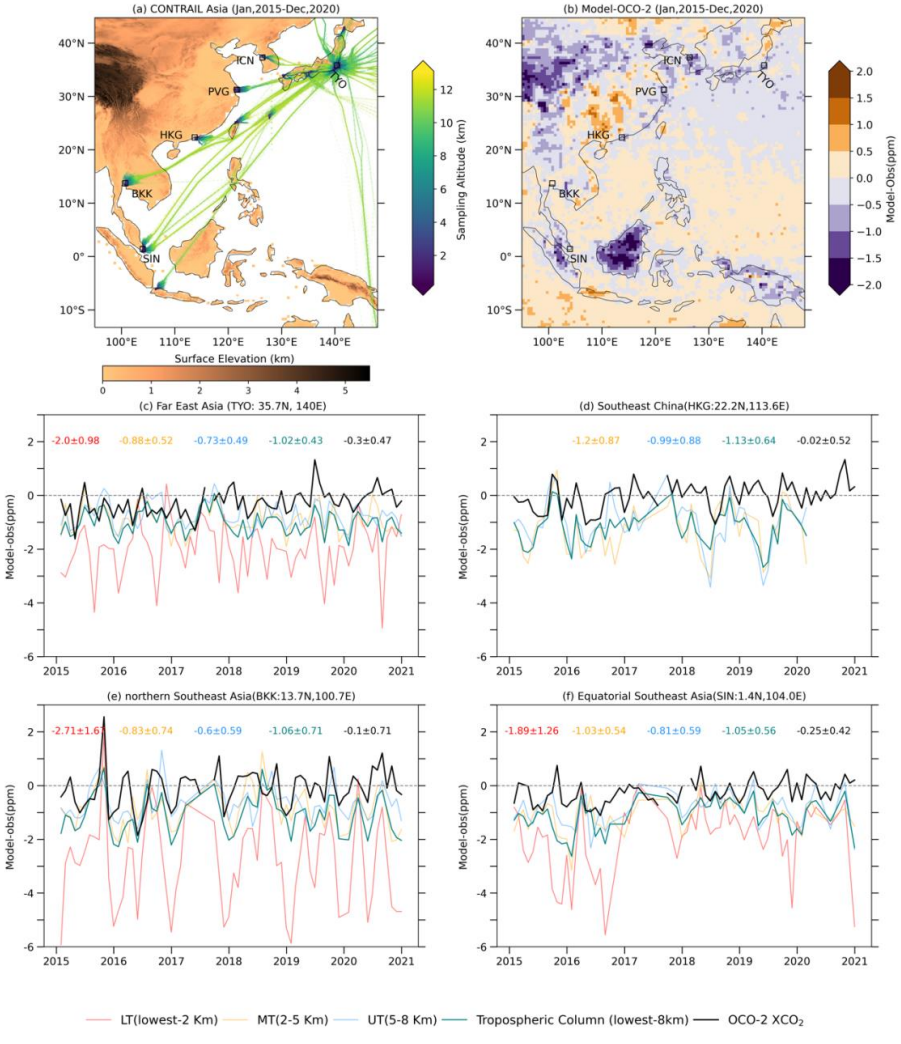

Figure 6: (a) CONTRAIL aircraft sampling locations with associated colours represent sampling altitude in km over Asia regions with surface elevation in km. There are four defined regions, each associated with specific airports, covering various vertical zones of carbon dioxide (CO_2) profiles. Far East Asia consisting of two airports, HND, NRT merged to prepare TYO, Southeast China with one airport HKG, northern Southeast Asia with one airport BKK, and equatorial Southeast Asia encompassing one airport SIN. (b) mean model-OCO2 XCO_2 differences over sampling locations during the mentioned period. (c), (d) (e), and (f) are time series of model-observation CO_2 differences over representative airports at different vertical depths of troposphere MT, LT and tropospheric column and XCO_2 utilising aircraft measurement and OCO-2. The numbers inside the (c), (d), (e), and (f) panels represent the mean and 1-σ standard deviation (STDEV) of model-observation difference over the period.